THE ASTROPHYSICAL JOURNAL, 452:634–651, 1995 October 20

CHEMICAL EVOLUTION OF THE ORION ASSOCIATION. III. THE LITHIUM ABUNDANCE OF F AND G STARS

KATIA CUNHA,[1] VERNE V. SMITH,[2] AND DAVID L. LAMBERT[2]
Received 1995 February 14; accepted 1995 May 1

ABSTRACT

We derive lithium abundances for a sample of 25 late F to early G dwarfs in the direction of the Orion association from spectra obtained with the McDonald Observatory's 2.1 m telescope plus a Cassegrain cross-dispersed echelle spectrometer at a spectral resolution of 60,000. Iron abundances are also derived for the slowly rotating stars. A kinematical discussion, combined with information on rotation and X-ray emission for the stars, led us to conclude that 10 stars in our sample are members of the Ic and Id subgroups of Orion, while two are probable members of the Ib subgroup, with the remaining stars being field stars in the direction of Orion. The Li abundances obtained for the seven members of the Ic subgroup with $v \sin i > 20$ km s^{-1} show a small scatter, comparable to our uncertainties in the abundance determinations themselves. The mean non-LTE Li abundance for the rapidly rotating Ic members is log ϵ(Li) = 3.2 $\pm$ 0.1—very close to the solar system meteoritic value of 3.3. If the Orion interstellar gas is representative of local Galactic gas, there is apparently little evidence of an increase in the Li abundance over the last 5 Gyr.

Subject headings: open clusters and associations: individual (Orion OB1) — stars: abundances — stars: evolution — stars: rotation

1. INTRODUCTION

Lithium depletion in main-sequence stars is far from being completely understood. Observations of Galactic clusters, where stellar luminosities, ages, and masses can be estimated, provide crucial clues to sorting out different mechanisms for the destruction of Li in main-sequence, or even pre–main-sequence (PMS), stars. The nearby clusters have historically provided an increasingly rich picture of the behavior of the Li abundance in young stars. Three of the key open clusters are α Per, the Pleiades, and the Hyades, with ages of roughly 50, 80, and 600 Myr, respectively. A sample of studies of lithium would include Cayrel et al. (1984), Boesgaard & Tripicco (1986), or Boesgaard, Budge, & Ramsey (1988) for the Hyades; Duncan & Jones (1983) and Boesgaard et al. (1988) for the Pleiades; and Balachandran, Lambert, & Stauffer (1988) for α Per. In this paper we discuss the lithium abundances of stars in the Orion association, a cluster of stars even younger than those in α Per.

The Orion association, one of the nearer regions of young stars with continuing large-scale star formation, is an attractive site for studying very young low-mass stars. Stars with masses less than about 2.0–2.5 $M_\odot$ are still collapsing toward the main sequence and can provide a window into the behavior of Li in the very earliest phases of stellar evolution. King's (1993) analysis of low-resolution spectra yielded Li abundances for a sample of 23 cooler ($T_{\rm eff} < 6100$ K) stars in the Orion Ic association and provided evidence for an order of magnitude spread in the Li abundances. He also found a suggestive pattern of lower Li abundances in those stars with the lowest values of projected rotational velocities ($v \sin i$). Some of these slowly rotating Li-depleted stars may not be members of the Orion association, so the question of the reality of a spread in Li abundance, plus a possible correlation with $v \sin i$, is still an open one. Here we report on Li abundances derived from high-resolution spectra for a different sample of stars in the direction of the Orion association: only three of our 25 stars were observed by King. We investigate, in detail, effective temperatures, surface gravities, rotational velocities, Fe abundances, and Li abundances, while addressing the critical question of membership for the sample of stars.

2. OBSERVATIONS

In this study we analyze high-resolution spectra for a sample of F and G dwarfs in the direction of the Orion association. The observations were obtained with the 2.1 m telescope of the McDonald Observatory plus the Cassegrain cross-dispersed Sandiford echelle spectrometer (McCarthy et al. 1993) and a Reticon 1200 × 400 pixel CCD detector. The spectra were obtained at a 2 pixel resolution of about $R = 60{,}000$ with complete wavelength coverage from 6100 to 7900 Å. A projected 2 pixel slit on the CCD corresponds to 1.″1 on the sky.

The observed spectra were reduced in a standard way using NOAO's IRAF data package, and the reduction consisted basically of the following steps: raw CCD images were corrected for bias levels by subtracting average bias frames for each night; scattered-light corrections were made by fitting two-dimensional smooth functions to the interorder light; an internal quartz lamp was used as a flat-field source for division of the frames. The resultant frames were then extracted to one-dimensional orders and placed on an absolute wavelength scale using a spectrum of a Th-Ar hollow cathode. In Figure 1 we show sample spectra for three stars: P1590, HD 294302, and P1455 in the region around the Li I doublet (6707 Å); the prominent features which appear in the spectra are identified, as well as two of the Fe I lines which were considered in this study.

The Orion association consists of four subgroups (Ia, Ib, Ic, and Id) of different locations, sizes, and ages, suggesting that

[1] Observatório Nacional, Rua General José Cristino 77, 20921 São Cristóvão, Rio de Janeiro, Brazil.
[2] Department of Astronomy and McDonald Observatory, University of Texas, Austin, TX 78712.

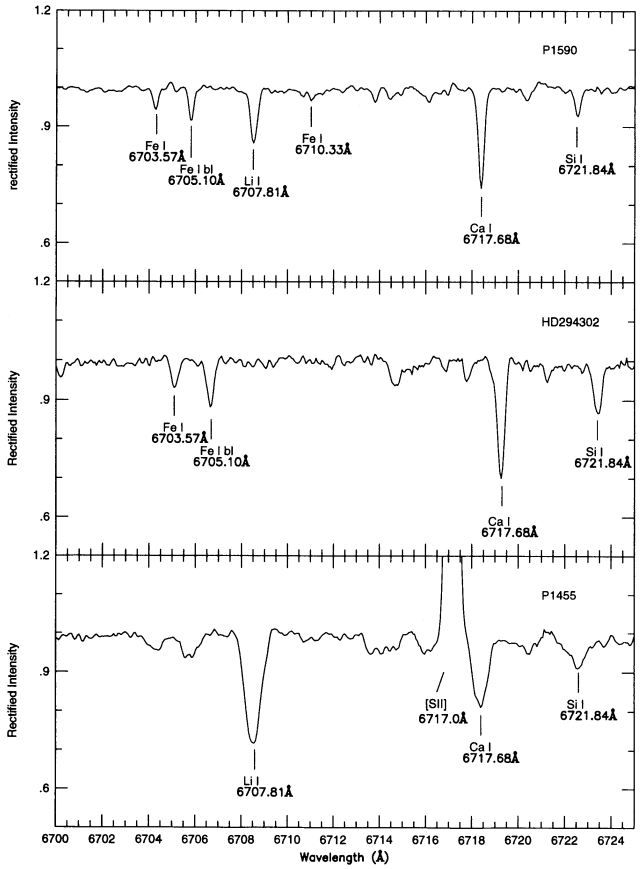

FIG. 1.—Sample spectra of the stars P1590, HD 294302, and P1455 in the region of the Li I resonance doublet. The most prominent features in these spectra are also identified. Note the [S II] emission in P1455: this emission arises from the Orion Nebula.

progressive star formation has occurred in the association, Ia being the oldest and Id the youngest subgroup. These subgroups were first identified by Blaauw (1964) and later by Warren & Hesser (1978), who carried out a detailed photometric study of the association, assigning the following ages (in millions of years) to the subgroups: 7.9 (Ia), 5.1 (Ib), 3.7 (Ic), and less than 0.5 (Id). More recently, Brown, de Geus, & de Zeeuw (1994) have presented a study based on VBLUW photometry and suggest that, contrary to the previous studies, the subgroup Ic is younger than Ib. However, the errors in the estimated ages for these two subgroups are such that they could actually overlap. Our observed sample consists of 25 stars between spectral types F6 and G3 in the direction of the Orion association, with stars drawn mainly from the list of Orion Ib, Ic, and Id members in Warren & Hesser (1978). Additional stars were also obtained from Parenago (1954). The program stars are listed in Table 1 by their HD or Parenago number, plus subgroup membership, V magnitudes, and Strömgren β measurements (all taken from Warren & Hesser 1978, except for seven stars, for which data were obtained using the SIMBAD database). In this table we also comment on the shape of the observed Hα profiles and present the estimated signal-to-noise ratio (S/N) of the spectra and dates of the observations. The S/N refers to the continuum around 6710 Å.

Although the late F and G stellar members of the Orion association are very young, having probably not yet arrived on the main sequence, most show photospheric absorption Hα profiles (typical of a star on or near the main sequence). In a few cases we identify a weak stellar emission in the core of the absorption line. The observed stellar emissions corresponded typically to a FWHM of about 0.4 Å and represent only a minor contribution to the profile. One star, however, showed a quite different shape for Hα: P1953. This star had much more complex Hα profile composed of a very broad stellar emission plus a large absorption (Fig. 2). In Figure 2 we plot three sample Hα profiles. Nebular Hα components, as well as in some cases [N II] and [S II] emission lines, were identified in the spectra of some stars.

In Figure 3 we present the positions of our target stars in the direction of Orion: the observed stars with absorption (stellar) features are represented by open circles, while the observed stars which showed strong Hα nebular emission are represented by open triangles. In this figure we indicate by filled circles the brightest stars which can be found in the Orion region (the three stars from the "belt" plus θ and ι Ori). The boundaries of the Ib and Ic subgroups are also sketched, with the Id subgroup (the Trapezium cluster) lying within Ic.

The stars observed in this program were chosen on the criterion that they were considered members of the different Orion subgroups by Warren & Hesser (1978). But we also

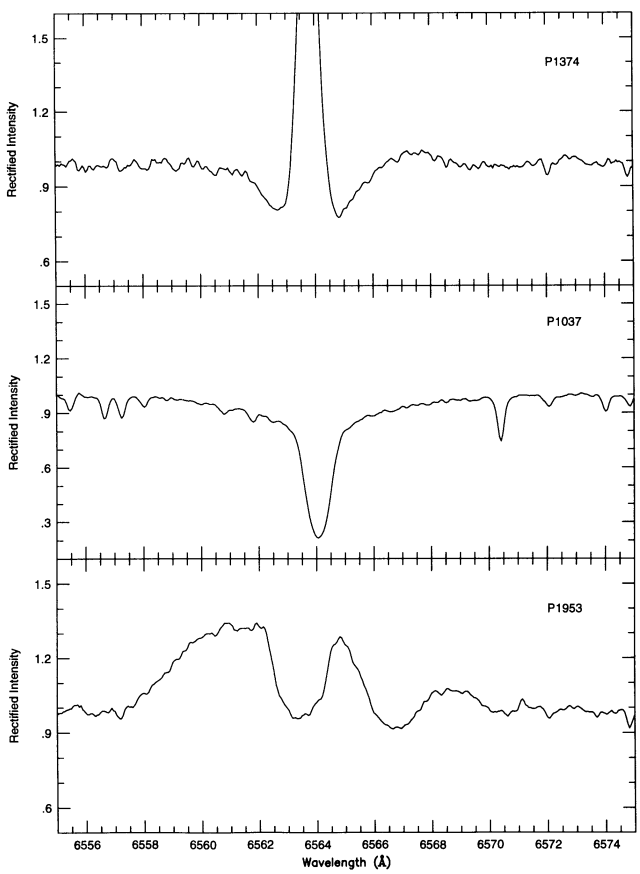

FIG. 2.—Sample spectra of the stars P1374, P1037, and P1953 in the region around the Hα line. We have chosen these stars to illustrate the different types of observed profiles: P1374 shows a rapidly rotating photospheric absorption line upon which is superimposed nebular Hα from the Orion gas. P1037 has a pure absorption profile, while P1953 shows complex stellar emission and absorption.

TABLE 1

PROGRAM STARS

Star	Subgroup	V	Strömgren β	Hα[a]	S/N	Date
P1037	Ic*	10.30	...	stel abs	200	1994 Jan 1
P1158	Ic	10.94	2.553	stel abs (+neb ems)	190	1994 Jan 2
P1179	Ic	11.47	2.601	stel abs (+small stel ems)	165	1993 Mar 3
P1199	Ic	10.68	2.543	stel abs (+neb ems)	280	1994 Jan 2
P1374	Id	10.31	2.661	neb ems (+stel abs)	120	1993 Feb 12
P1455	Id	10.92	2.497	neb ems (+stel abs)	180	1994 Jan 1
P1467	Ic*	10.56	...	stel abs	340	1993 Dec 31
P1474	Ic*	10.96	...	stel abs	230	1993 Dec 31
P1590	Ic	10.27	2.584	stel abs	130	1993 Feb 12
P1626	Ic	11.23	2.512	stel abs (+neb ems)	120	1993 Mar 4
P1657	Ic	11.49	2.611	stel abs	160	1993 Mar 4
P1662	Ic	10.72	2.567	stel abs (+small neb ems)	330	1993 Mar 6
P1789	Ic	10.55	2.615	stel abs (+small stel ems)	200	1993 Mar 4
P1953	Ic	9.87	2.568	complex stel (ems + abs)	200	1993 Feb 12
P1955	Ic	10.91	2.575	neb ems + stel (abs + ems)	120	1994 Jan 2
P2125	Ic*	10.52	...	stel abs (+small neb ems)	190	1994 Jan 1
P2267	Ic	11.38	2.571	stel abs (+small neb ems)	90	1993 Mar 3
P2339	Ic*	9.96	...	stel abs	320	1994 Jan 1
P2374	Ic*	10.92	...	stel abs	140	1993 Dec 31
P2909	Ic*	11.6	...	stel abs	235	1993 Dec 31
HD 36235	Ic	9.45	...	stel abs	250	1993 Feb 10
HD 294269	Ib	10.68	2.573	stel abs	180	1993 Feb 12
HD 294297	Ib	10.12	2.634	stel abs	200	1992 Nov 7
HD 294298	Ib	10.80	2.578	stel abs (+small stel ems)	180	1993 Feb 10
HD 294302	Ib	11.45	2.556	stel abs (+small neb ems)	150	1994 Jan 2

NOTE.—See text for explanation of asterisks.

[a] Abbreviations used are as follows: stel abs ≡ stellar absorption line; stel ems ≡ stellar emission line; neb ems ≡ nebular emission line.

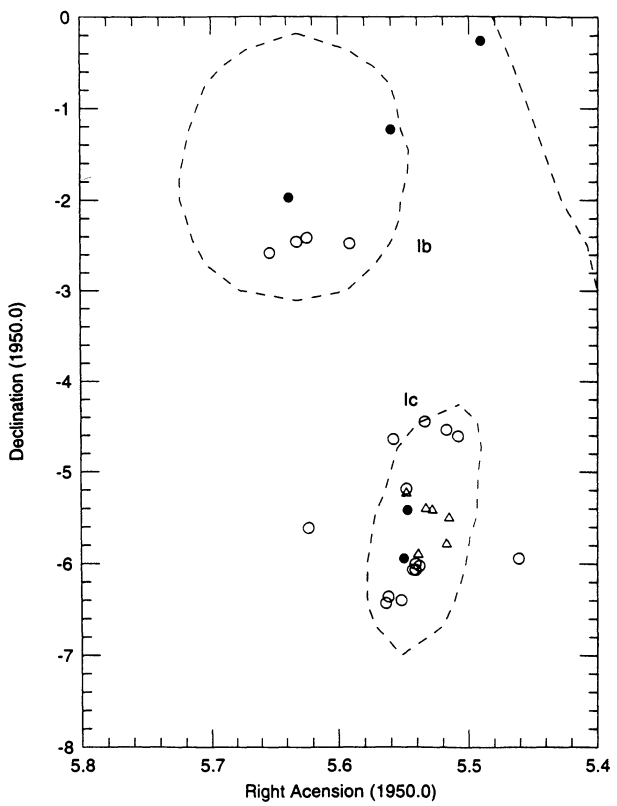

FIG. 3.—Positions of the observed stars in the Orion region. The boundaries of subgroups Ib and Ic are sketched. The target stars which show nebular emission lines in the spectra are represented by open triangles, while those with no emission lines are shown as open circles. The brightest stars in the Orion region are also represented (*filled circles*).

included seven other stars from Parenago (1954) which fall within the boundaries of the Ic subgroup: the seven are marked with asterisks in Table 1.

3. ORION ASSOCIATION MEMBERSHIP

Contamination of the sample by field stars will hamper a search for correlation between a star's lithium abundance and other characteristics, such as the iron abundance, effective temperature, and rotational velocity. Therefore, an assessment of membership in the Orion association is crucial. In this section we use as much kinematic information as possible (the radial velocities, proper motions, and distance to the Orion association) to determine which stars in our sample are "probable" or "certain" Orion members and which are field stars.

As a start, we note that the radial velocity of the Orion association is well defined; according to Warren & Hesser (1978), the velocities of the Orion members fall within the range of $V_r = +23 \pm 8$ km s^{-1}. Based upon our radial velocity measurements presented in Table 2, nine stars are immediately rejected: P1037, P1158, P1199, P1474, P1662, P2125, P2267, HD 294269, and HD 294302. Although these stars may be binary systems, we can find no evidence of a secondary spectrum down to a few percent of the continuum, and we consider it unlikely that the radial velocities are perturbed significantly by an unseen companion.

Evidence regarding membership is also provided by proper motions, and the Orion region is a well-studied area in this regard. There are several recent proper-motion studies, mostly centered on the Ic subgroup near the Trapezium, and these are by McNamara (1976), McNamara & Huels (1983), van Altena et al. (1988), Jones & Walker (1988), and McNamara et al. (1989). These studies have internal accuracies ranging from

about 0.2 mas yr^{-1} for the van Altena et al. (1988) study, to approximately 0.5–1 mas yr^{-1} (Jones & Walker 1988; McNamara et al. 1989), to ~1 mas yr^{-1} for McNamara (1976) and ~3 mas yr^{-1} for McNamara & Huels (1983); the last two studies are based upon a reanalysis of the older Parenago (1954) and Strand (1958) data, respectively. Nineteen of the stars observed here have proper motions tabulated in McNamara et al. (1989), but the other studies contain only a few of our stars, thus we use the McNamara et al. (1989) study as the main source of the proper motions. A comparison of stars in common with the McNamara et al. (1989) study with stars from van Altena et al. (1988), Jones & Walker (1988), and McNamara (1976) which are also studied here yields 14 proper-motion measurements in common. The average difference in total proper motion [$\mu_T = (\mu_x^2 + \mu_y^2)^{1/2}$] and standard deviation derived among these various studies is $\Delta\mu_T = -0.8 \pm 2.6$ mas yr^{-1}, thus, combining and comparing absolute proper motions from the literature of stars observed here probably results in uncertainties of perhaps 3 mas yr^{-1} (a conservative estimate). All of the studies mentioned above find a very small mean proper motion for Orion members.

In Table 2 we list the proper motions (when available) for the stars observed here. The radial velocities and proper motions can now be combined to yield powerful constraints on Orion membership; in Figure 4 we plot our derived radial velocities versus total proper motion, μ_T in mas yr^{-1}. The stars observed here fall into three categories: (1) 10 stars with large proper motions ($\geq$20 mas yr^{-1}), most of which have radial velocities clearly incompatible with Orion membership; (2) a group of four stars with $\mu_T \sim 6$–10 mas yr^{-1} but having radial velocities consistent with membership; and (3) a larger group (eight) with small proper motions ($\mu_T \leq 3$ mas yr^{-1}) and radial velocities appropriate for membership.

Orion presents a particularly simple situation because the molecular cloud effectively obscures distant background stars; thus most stars are either Orion members or field stars lying between us and Orion. At a distance $D = 440$ pc (distance to Ic; Warren & Hesser 1978), a proper motion of 1 mas yr^{-1} corresponds to 2.1 km s^{-1} in transverse radial velocity, V_T. Thus, in Figure 4 we interpret the stars with $\mu_T \geq 20$ mas yr^{-1} as nonmembers and those with very small proper motions ($\mu_T \leq 3$ mas yr^{-1}; all of them have the V_r of the Orion association) as certain members. The small group of stars with $\mu_T \sim 6$–10 mas yr^{-1} and having radial velocities consistent with the Orion members are more problematic. If we accept the fact that all Orion members must have very small proper motions (1 σ corresponding to roughly 3 mas yr^{-1}), then we reject these stars as members. However, it must also be noted that the Orion region, especially Orion Ic, is a site of very recent star formation with the possibility that dynamic processes resulting from star formation in a dense environment may influence the stellar motions (e.g., star-star, star-binary, or binary-binary interactions, or supernova explosions). In fact, based on their analysis of proper motions of stars near the region of Orion Ic, Jones & Walker (1988) conclude that the stars in the Orion association do not represent a protocluster but a system in disruption, as originally suggested by Blaauw (1964). At the distance of the Orion association, the variations in radial velocity of $\pm$8 km s^{-1} noted by Warren & Hesser (1978) would correspond to proper-motion variations of $\pm$3.8 mas yr^{-1}, if this motion were projected perpendicular to our line of sight. From the stars we consider to be members (Table 2) we derive a mean radial velocity of $+21 \pm 6$ km s^{-1}. This is in good agreement with both Blaauw (1991) (from proper-motion dispersions) and Warren & Hesser (1978) estimates. The internal velocity dispersions typical of OB associations range from 2–6 km s^{-1} (Blaauw 1991).

The combination of radial velocity with small proper motion indicates that the stars P1179, P1374, P1455, P1626, P1657, P1789, P1953, and P1955 should be considered definite

TABLE 2

STELLAR KINEMATICS AND MEMBERSHIP

STAR	PROPER MOTION (mas yr^{-1}) μ_x	μ_y	R_v	X-RAY	MEMBERSHIP
P1037	+71.52	+30.06	+46.7		No
P1158	−26.70	−63.48	−37.4		No
P1179	+1.70	+0.32	+20.8		Yes
P1199	−48.20	−84.07	−10.1		No
P1374	−1.17	+2.47	+12.5		Yes
P1455	−1.80	+0.75	+23.0		Yes
P1467	−14.88	−29.12	+24.3		No
P1474	+20.54	−24.02	−11.9		No
P1590	−1.60	+6.79	+23.8	No	No
P1626	+1.04	+1.16	+20.9	No	Yes
P1657	+0.62	−0.09	+29.2		Yes
P1662	−12.26	+28.43	+81.9		No
P1789	+1.17	+1.38	+23.3		Yes
P1953	+1.16	+0.79	+30.8		Yes
P1955	+0.99	+0.04	+18.1	Yes	Yes
P2125	+36.73	+12.24	+74.7		No
P2267	+2.07	+18.35	+56.0		No
P2339	−0.50	+6.88	+19.4	Yes	Yes
P2374	+4.97	−7.08	+21.1	Yes	Yes
P2909	+25	−11	+15.4		No
HD 36235	−30.0	−4.0	+17.2		No
HD 294269	...	...	+72.8		No
HD 294297	+10.5	−1.8	+25.0		Probable Yes
HD 294298	...	...	+11.5		Probable Yes
HD 294302	...	...	+62.3		No

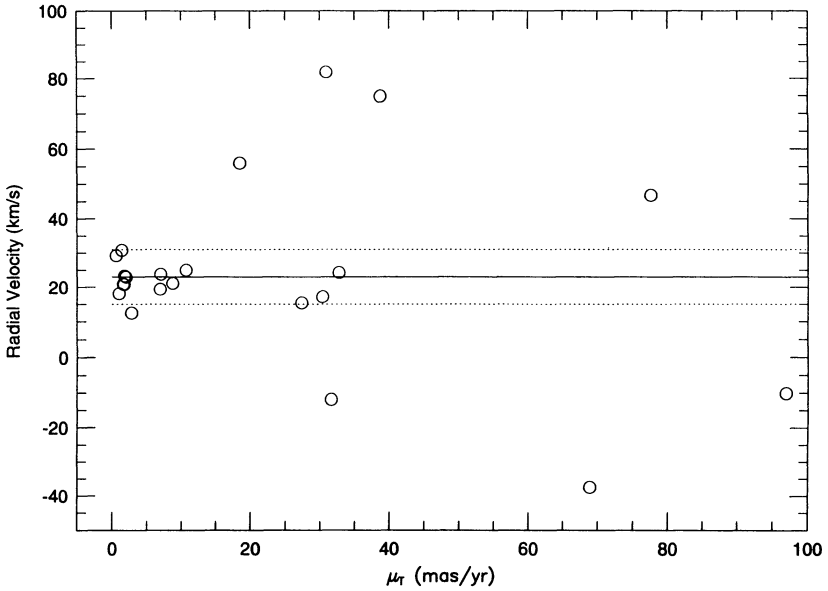

FIG. 4.—Radial velocities measured here vs. proper motions from the literature. Note the large spread in V_r for those stars with $\mu_T \geq 20$ mas yr^{-1}: these are the nonmembers. All stars with $\mu_T \leq 10$ mas yr^{-1} have radial velocities which coincide with Orion membership. The solid and dotted lines are mean and limiting V_r values for Orion members as discussed in Warren & Hesser (1978).

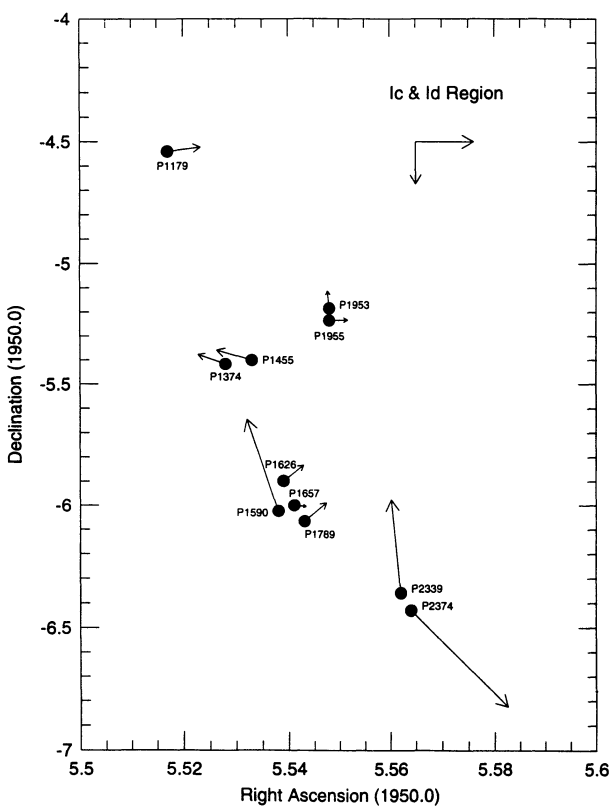

FIG. 5.—Positions and proper motions of possible subgroup Ic and Id members. The arrows indicate the proper motions, with the scale set by the pair of orthogonal arrows, which illustrate motions of 3 mas yr^{-1} in right ascension and declination, respectively. All stars shown here have radial velocities in agreement with Orion association membership. Based upon other criteria (X-ray emission and v sin i), we finally reject P1590 from membership status.

members. The four stars with $\mu_T \sim 6$–10 mas yr^{-1} and radial velocity coincident with association membership (P1590, P2339, P2374, and HD 294297) we consider as tentative members on the basis of the kinematical evidence.

Another test for membership in a young association, such as Orion, is the presence of X-ray emission. Lack of X-ray emission does not necessarily disqualify a star from status as a young member, but the presence of X-rays from stars that are not members of close binary systems is suggestive of youth. Smith, Pravdo, & Ku (1983) from *Einstein* observations of a number of post–T Tauri G stars in the direction of Orion Ic found that rapidly rotating young stars (past the T Tauri phase) often have stronger X-ray emission than T Tauri stars. In Table 2 we indicate which stars studied here were observed by Smith et al. and which exhibit or lack detectable X-ray emission. The definite, rapidly rotating member P1955 is detected at $L_X/L_{bol} \approx 2 \times 10^{-4}$. The definite nonmembers P1662 and P2125 are not detected. Curiously, the definite member P1626 is not detected, although Smith et al. (1983) point out that stars with evidence of extensive circumstellar disks may lack X-ray emission due to absorption, in the near-stellar environment, of any X-rays generated by the young star. We note also that the questionable membership star P1590 is not detected.

Both P2339 and P2374 are detected X-rays sources with $L_X/L_{bol} \approx 4 \times 10^{-5}$ and 3×10^{-4}, respectively. These are significant detections because both stars were rejected as members by King (1993) on the basis of their proper motions (see also Table 2). X-ray emission plus radial velocity suggest that both stars are members of the Orion association.

In Figure 5 we plot the positions of the certain and possible members of Orion Ic within 2.5 deg^2 centered approximately on the Trapezium. The radial velocities of both P2339 and P2374 are, within our uncertainties of about ± 1.5 km s^{-1}, identical, and their vector proper motions are directed within

30° of being in opposite directions: within the uncertainties of the proper motions, distances, and radial velocities, these two stars could easily have space motions directed 180° apart. Their distance apart on the sky is 280″, which, at a distance of 440 pc, corresponds to a linear separation of 0.6 pc. With estimated space motions of 26 ± 2 km s^{-1} for both stars, and assuming a current separation of 0.6 pc, P2339 and P2374 would have been in close proximity some 11,000 years ago.

The data on X-ray emission for the stars considered as tentative members on the basis of their kinematics suggests that we reject P1590 from membership, but that P2339 and P2374 should be considered as Orion Ic members. The stars HD 294297 and HD 294298 are probable Orion Ib members (Warren & Hesser 1978). HD 294297 is one of the four stars with $\mu_T \sim 6$–10 mas yr^{-1}; however, the source for the proper motion is the SAO catalog, and Warren & Hesser suggest caution in giving much weight to such a small proper motion from this catalog. Concerning HD 294298, it is one of only five stars in our sample with detectable stellar Hα emission and we use this as a criterion for continued inclusion as a probable member.

In the next section we discuss lithium abundances, projected rotational velocities, and iron abundances for the stars considered to be Orion members, and we discuss further how the Li and Fe abundances plus projected radial velocities and derived surface gravities may provide additional evidence on membership in the association.

4. ANALYSIS

4.1. *Spectral Line Selection*

Crucial to the determination of fundamental stellar parameters (effective temperature, surface gravity, and microturbulence), and the derived abundances, is the choice of spectral lines. In this paper we are concentrating on studying lithium abundances in F and G dwarf members of the Orion association, and we have chosen to use Fe I and Fe II lines to determine $T_{\rm eff}$ and log g as well as to define an Fe abundance. Our derivation of the stellar parameters for the stars will be discussed in § 4.2. The sample stars are restricted in spectral types to late F to early G, and therefore are not very different from the Sun in $T_{\rm eff}$, log g, or metallicity; thus it is possible to tie our analysis closely to solar parameters.

Meylan et al. (1993) provide a critically evaluated list of spectral lines suitable for high-quality abundance analyses in solar-like stars. They have fitted Voigt profiles to a large number of spectral lines in the Kurucz et al. (1984) solar flux atlas from the McMath solar telescope and Fourier transform spectrometer, and list the equivalent widths of these lines. Starting from this list, we compiled a subset of Fe I and Fe II lines that appeared unblended and measurable in our echelle spectra of the stars and the asteroid 1 Ceres, taken along with our Orion stars as a proxy solar spectrum which mimics the quality of the program stellar spectra. A very broad absorption feature has been identified in the reflectance spectrum of Ceres ranging from 5700 to 8000 Å, with a minimum near 6000 Å (Vilas et al. 1993). However, this feature is extremely weak (less than 1% deep at maximum) and very extended (much wider than our echelle orders) and therefore it has no effect on our equivalent width measurements. Our McDonald spectra begin near 6090 Å, and we cut off the line list at the beginning of the atmospheric O_2 "*B* band" to avoid telluric contamination, both at the *B* band and farther to the red. Within this interval we identified 52 Fe I and six Fe II lines deemed measurable in Sandiford echelle spectra of solar-type stars. These lines are listed in Table 3: wavelengths are taken from Meylan et al. (1993), while transition and multiplet designations are from Fuhr, Martin, & Wiese (1988) or Moore (1945).

We have measured the equivalent widths (W_λ) of this selected sample of Fe lines for all target stars which were rotating

TABLE 3

Fe TRANSITIONS

Line	Transition	RMT[a] Number	χ (eV)	log gf
Fe I λ6093.644	$y\ ^3F^o$–$f\ ^5P$	1177	4.61	−1.363
Fe I λ6094.374	$y\ ^3F^o$–$f\ ^5P$	1177	4.65	−1.577
Fe I λ6096.665	$z\ ^3F^o$–$e\ ^3F$	959	3.98	−1.766
Fe I λ6105.131	$y\ ^3F^o$–$g\ ^5F$	1175	4.55	−1.937
Fe I λ6151.618	$a\ ^5P$–$y\ ^5D^o$	62	2.18	−3.335
Fe I λ6165.360	$c\ ^3F$–$v\ ^3G^o$	1018	4.14	−1.498
Fe I λ6173.336	$a\ ^5P$–$y\ ^5D^o$	62	2.22	−2.842
Fe I λ6180.204	$a\ ^3G$–$y\ ^3D^o$	269	2.73	−2.655
Fe I λ6187.990	$z\ ^3F^o$–$e\ ^3F$	959	3.94	−1.569
Fe I λ6200.313	$b\ ^3F2$–$y\ ^3F^o$	207	2.61	−2.372
Fe I λ6213.430	$a\ ^5P$–$y\ ^5D^o$	62	2.22	−2.656
Fe I λ6220.784	$z\ ^3F^o$–$e\ ^5F$	958	3.88	−2.307
Fe I λ6226.736	$z\ ^3D^o$–$e\ ^5F$	981	3.88	−2.083
Fe I λ6229.228	$b\ ^3P$–$y\ ^3D^o$	342	2.84	−2.966
Fe I λ6240.646	$a\ ^5P$–$z\ ^3P^o$	64	2.22	−3.308
Fe I λ6297.793	$a\ ^5P$–$y\ ^5D^o$	62	2.22	−2.750
Fe I λ6322.686	$b\ ^3F2$–$y\ ^3F^o$	207	2.59	−2.345
Fe I λ6330.850	$y\ ^3D^o$–$h\ ^5D$	1254	4.73	−1.154
Fe I λ6335.331	$a\ ^5P$–$y\ ^5D^o$	62	2.20	−2.364
Fe I λ6392.539	$a\ ^3P$–$y\ ^5D^o$	109	2.28	−3.993
Fe I λ6436.407	$c\ ^3F$–$v\ ^3D^o$	1016	4.19	−2.367
Fe I λ6481.870	$a\ ^3P$–$y\ ^5D^o$	109	2.28	−2.959
Fe I λ6498.939	$a\ ^5F$–$z\ ^7F^o$	13	0.96	−4.658
Fe I λ6518.367	$b\ ^3P$–$y\ ^3D^o$	342	4.73	−2.469
Fe I λ6591.313	$d\ ^3F$–$t\ ^3D^o$	1229	4.59	−1.877
Fe I λ6593.870	$a\ ^3H$–$z\ ^5G^o$	168	2.43	−2.364
Fe I λ6608.026	$a\ ^3P2$–$y\ ^5D^o$	109	2.28	−3.981
Fe I λ6627.545	$y\ ^3F^o$–$g\ ^5D$	1174	4.55	−1.507
Fe I λ6646.932	$b\ ^3F2$–$z\ ^3G^o$	206	2.61	−3.929
Fe I λ6667.419	$a\ ^3H$–$z\ ^5G^o$	168	2.45	−4.031
Fe I λ6703.567	$a\ ^3G$–$y\ ^3F^o$	268	2.76	−3.033
Fe I λ6710.320	$a\ ^3F$–$z\ ^5F^o$	34	1.48	−4.851
Fe I λ6725.357	$y\ ^5D^o$–$e\ ^3F$	1052	4.10	−2.202
Fe I λ6726.667	$y\ ^5P^o$–$e\ ^5P$	1197	4.59	−1.005
Fe I λ6732.065	$d\ ^3F$–$u\ ^3G^o$	1225	4.58	−2.230
Fe I λ6733.151	$y\ ^5P^o$–$g\ ^5D$	1195	4.64	−1.469
Fe I λ6745.101	$d\ ^3F$–$x\ ^1D^o$	1227	4.58	−2.114
Fe I λ6745.956	$c\ ^3F$–$w\ ^5G^o$	1005	4.08	−2.767
Fe I λ6750.152	$a\ ^3P2$–$z\ ^3P^o$	111	2.42	−2.642
Fe I λ6752.707	$y\ ^5P^o$–$g\ ^5D$	1195	4.64	−1.235
Fe I λ6793.259	$c\ ^3F$–$w\ ^5G^o$	1005	4.08	−2.389
Fe I λ6806.845	$a\ ^3G$–$y\ ^3F^o$	268	2.73	−3.126
Fe I λ6810.263	$y\ ^5P^o$–$e\ ^5P$	1197	4.61	−0.894
Fe I λ6828.591	$y\ ^5P^o$–$g\ ^5D$	1195	4.64	−0.755
Fe I λ6833.226	$y\ ^5P^o$–$e\ ^3D$	1194	4.64	−1.926
Fe I λ6837.006	$d\ ^3F$–$u\ ^3G^o$	1225	4.59	−1.718
Fe I λ6839.830	$b\ ^3F2$–$z\ ^5G^o$	205	2.56	−3.367
Fe I λ6843.656	$y\ ^3F^o$–$e\ ^3D$	1173	4.55	−0.733
Fe I λ6855.162	$y\ ^5P^o$–$g\ ^5D$	1195	4.54	−0.511
Fe I λ6857.250	$c\ ^3F$–$z\ ^1G^o$	1006	4.08	−2.080
Fe I λ6861.942	$a\ ^3P2$–$y\ ^5D^o$	109	2.42	−3.806
Fe I λ6862.491	$y\ ^5P^o$–$e\ ^7G$	1191	4.56	−1.413
Fe II λ6084.111.....	$a\ ^4G$–$z\ ^6F^o$	46	3.19	−3.840
Fe II λ6149.258.....	$b\ ^4D$–$z\ ^4P^o$	74	3.87	−2.750
Fe II λ6239.953.....	$b\ ^4D$–$z\ ^4P^o$	74	3.87	−3.405
Fe II λ6247.557.....	$b\ ^4D$–$z\ ^4P^o$	74	3.87	−2.244
Fe II λ6446.410.....	$c\ ^4F$–$x\ ^4G^o$	199	6.20	−1.942
Fe II λ6456.383.....	$b\ ^4D$–$z\ ^4P^o$	74	3.89	−1.967

[a] Revised multiplet table (see Moore 1945).

slowly enough ($v \sin i < 25$ km s^{-1}) so that most spectral lines were free of blends and readily measurable. These W_λ values were measured with the IRAF data package by straight numerical integration. Our measured W_λ values for the stars are listed in Tables 4 and 5, respectively, for our sets of Fe I and Fe II lines. In Tables 4 and 5 an entry consisting of ellipsis dots (...) indicates that the line was not measured, owing either to a blend or to the fact that it was very weak or not present in the spectrum; an entry "cr" indicates the presence of a cosmic ray in the exact location of the spectral line. We have chosen not to attempt to clean the cosmic rays in these cases, as this would impart larger errors to the W_λ measurements; also, since we are considering a large enough sample of Fe lines, the few lines disregarded would not lead to any significant degradation of the final abundances.

We have compared the equivalent width measurements from our Ceres spectrum with the equivalent widths measured by Meylan et al. (1993) from the solar flux atlas (Kurucz et al. 1984), in order to have some estimate of the quality of our measurements. The comparison of the equivalent widths in Figure 6 shows that they agree to within about 5 mÅ. Such a discrepancy is certainly within the uncertainties of our measurements, which we estimate as being not larger than a few mÅ, based upon the S/N and resolution of our spectra. In addition, there is some uncertainty in the continuum placement and the numerical limits of integration.

Our abundance analyses use the model atmospheres generated by the ATLAS9 code (R. L. Kurucz 1994, private communication): these are LTE, plane-parallel, line-blanketed models. The fact that the Orion stars have effective temperatures and surface gravities similar to those of the Sun suggests that use of the solar ATLAS9 model would be appropriate for deriving "solar" gf-values for the Fe I and Fe II lines. In this derivation we assume the Fe abundance log ϵ(Fe) = 7.51. Use of Meylan et al.'s W_λ values with a microturbulence of 1.0 km s^{-1} gives the gf-values in Table 3. These gf-values are systematically larger than those tabulated by Meylan et al.: $\Delta \log gf$(Table 3 − Meylan) = 0.03 ± 0.03. The small offset is probably due to differences in the adopted Fe abundances.

The assumed Fe abundance is the meteoritic value recommended by Anders & Grevesse (1989), who derived it by combining meteoritic measurements of ratios Fe/X with solar photospheric spectroscopic determinations of the ratios X/H for 12 elements. Anders & Grevesse noted that the spectroscopic Fe abundance was significantly higher than the meteoritic abundance: log ϵ(Fe) = 7.67 ± 0.03 (see Blackwell et al. 1986). With near-unanimity, more recent analyses of the solar Fe I and Fe II lines have put the spectroscopic Fe abundance equal to the meteoritic abundance to within the small errors of measurement; see Biémont et al. (1991), Holweger, Heise, & Kock (1990), Holweger et al. (1991), Hannaford et al. (1992), Holweger, Kock, & Bard (1995), and Milford, O'Mara, & Ross (1994). Thus, our adoption of the meteoritic abundance [log ϵ(Fe) = 7.51] would seem to be well justified.

There remains, however, a measure of uncertainty. In particular, Blackwell, Lynas-Gray, & Smith (1995) obtain the abundance log ϵ(Fe) = 7.64 ± 0.03 using a set of accurate laboratory gf-values, a thorough analysis of a set of carefully selected Fe I lines, and the Holweger & Müller (1974) empirical model solar atmosphere. (The several analyses referenced above also use this empirical atmosphere.) Analyzing Fe II lines with gf-values taken from Hannaford et al. (1992), Blackwell et al. (1995) obtain the abundance log ϵ(Fe) = 7.53, which is consistent with the meteoritic value but lower than that from the Fe I lines. When a Kurucz theoretical model is used, the Fe I and Fe II abundances are found to be 7.57 and 7.54, respectively; the Fe I − Fe II difference is effectively removed, and the mean abundance is only slightly higher than the meteoritic abundance. Thus, this analysis would seem to vindicate our calculation of the solar gf-values in Table 3. But Blackwell et al. observe that the theoretical model fails to reproduce observations of solar limb darkening of the continuum in the visible and near-infrared. On the other hand, the Holweger-Müller model, which was constructed to fit the limb-darkening observations, results in a "high" Fe abundance from Fe I lines

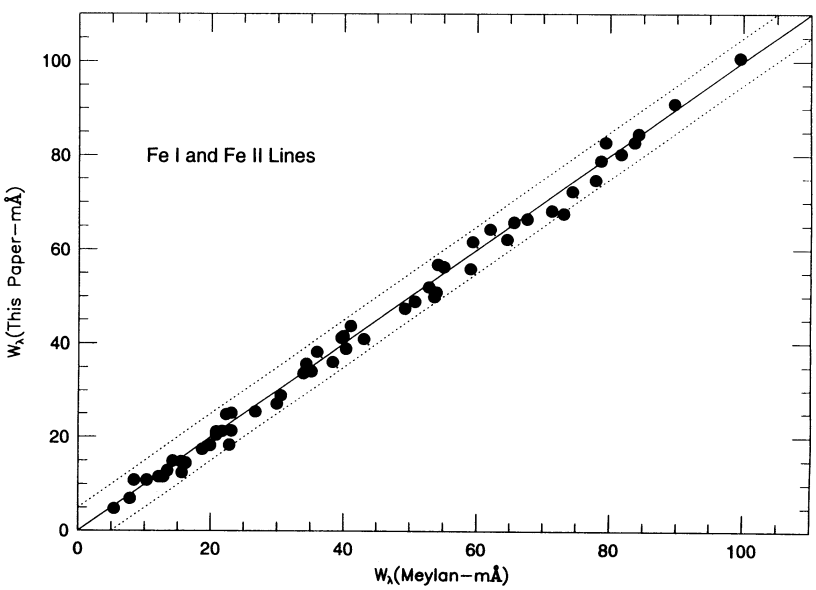

FIG. 6.—Comparison of the measured equivalent widths in our Ceres spectra with those measured by Meylan et al. (1993) from the solar atlas. The solid line indicates perfect agreement, while the dotted lines show ±5 mÅ.

TABLE 4

Fe I Equivalent Width Measurements (mÅ)

Star	Wavelength (Å)																	
	6093	6094	6096	6105	6151	6165	6173	6180	6187	6200	6213	6220	6226	6229	6240	6297	6322	6330
P1037	27	...	39	14	55	38	71	67	58	72	80	17	37	47	48	80	90	...
P1158	10	cr	25	...	23	17	40	18	18	39	54	cr	...	14	17	46	43	...
P1199	37	...	38	10	51	44	67	63	43	69	81	15	29	37	44	64	72	...
P1455	45	...	39	9	51	61	78	67	48	71	98	...	...	...	...	...	104	...
P1467	28	17	34	11	45	39	65	54	42	62	76	18	26	38	40	...	73	34
P1474	37	26	45	15	52	48	77	67	52	84	92	22	40	50	54	...	82	38
P1590	16	10	21	4	27	23	46	30	26	46	57	8	17	16	23	...	48	15
P1657	13	13	16	6	28	...	46	29	28	55	61	...	13	20	...	...	72	26
P1662	15	17	24	...	36	...	45	38	...	45	67	9	14	21	23	cr	55	...
P2125	22	15	26	9	38	39	53	54	33	61	72	10	25	31	36	...	72	27
P2267	26	28	42	...	...	41	70	47	51	73	77	14	24	39	44	...	73	...
P2339	23	19	30	9	40	32	60	47	40	68	76	...	18	29	88	...	70	23
P2374	33	20	33	13	47	41	65	50	42	71	80	12	25	36	42	...	68	33
P2909	42	29	50	19	64	56	85	78	72	90	92	25	43	56	65	...	96	42
HD 36235	...	10	14	...	22	19	37	29	20	39	...	6	12	16	20	...	46	14
HD 294269	...	...	50	13	60	49	92	66	55	94	98	26	41	53	61	94	90	47
HD 294297	...	...	...	...	...	...	...	...	...	...	...	...	...	...	...	79	...	...
HD 294302	...	18	28	...	44	39	71	48	45	cr	76	22	9	40	cr	89	68	...
Ceres	34	25	41	15	51	47	72	61	55	79	83	34	21	42	52	83	80	...
η Cas	19	13	25	8	35	32	52	45	33	57	63	22	10	42	52	61	57	22

Star	Wavelength (Å)																	
	6335	6392	6436	6481	6498	6518	6591	6593	6608	6627	6646	6667	6703	6710	6725	6726	6732	6733
P1037	103	15	...	...	55	71	16	...	25	25	13	...	35	19	18	40	...	28
P1158	63	...	...	35	cr	26	...	62	...	...	...	...	14	...	...	20	...	...
P1199	101	17	...	61	48	53	7	83	9	22	11	...	47	13	cr	57	8	25
P1455	114	...	19	80	...	...	...	98	16	28	13	12	30	18	18	49	...	...
P1467	92	9	12	63	39	56	16	84	15	26	9	4	33	17	15	48	8	20
P1474	112	20	12	77	43	86	12	93	21	30	7	...	47	14	20	55	15	32
P1590	74	11	8	37	17	37	...	62	5	12	...	...	17	6	6	27	...	10
P1657	80	...	...	63	20	61	6	65	7	...	...	...	14	...	...	28	...	...
P1662	88	7	...	42	35	cr	cr	66	...	11	...	...	27	...	14	38	...	13
P2125	92	14	8	66	36	51	8	74	10	20	7	7	24	12	12	43	8	20
P2267	85	12	8	...	40	50	15	99	20	26	9	6	35	17	17	44	8	19
P2339	89	5	7	55	41	...	9	75	13	24	5	6	27	18	13	47	5	21
P2374	96	16	10	62	43	68	11	85	14	28	11	6	33	16	16	50	7	23
P2909	113	23	...	81	62	70	18	104	28	40	17	11	56	30	25	58	9	37
HD 36235	74	...	...	31	29	...	...	58	...	...	...	...	11	...	...	19	...	8
HD 294269	114	42	15	93	71	74	16	103	29	38	19	...	55	38	31	cr	...	cr
HD 294297	...	...	...	44	21	37	6	70	7	23	...	...	25	8	6	27	6	22
HD 294302	95	17	...	74	30	...	10	85	...	22	...	...	32	...	...	57	...	...
Ceres	101	18	12	66	49	62	12	91	20	29	12	...	44	17	21	50	11	27
η Cas	79	9	6	49	31	48	8	75	12	18	4	4	23	8	9	36	5	18

Star	Wavelength (Å)															
	6745	6745	6750	6752	6793	6806	6810	6828	6833	6837	6839	6843	6855	6857	6861	6862
P1037	...	...	80	30	10	32	41	58	...	...	cr	65	68	20	17	cr
P1158	...	...	46	15	...	11	19	cr	...	...	cr	32	36	5	...	10
P1199	6	6	74	37	...	38	40	58	11	22	32	52	72	18	cr	24
P1455	...	...	83	...	...	37	55	79	...	28	...	...	...	...	...	...
P1467	7	...	69	38	11	30	41	53	10	19	26	65	76	20	20	32
P1474	13	11	85	41	20	38	60	66	15	21	36	70	79	24	19	36
P1590	...	...	52	...	8	15	21	29	...	9	11	36	49	10	6	17
P1657	...	...	57	22	...	17	31	47	...	...	21	43	51	...	...	...
P1662	...	...	54	26	...	...	31	37	...	...	22	36	57	13	...	cr
P2125	8	8	62	...	9	26	43	47	...	17	25	56	69	18	...	...
P2267	12	5	...	33	14	20	48	52	11	18	...	58	71	27	...	...
P2339	7	4	62	30	12	23	44	60	8	13	21	55	80	17	...	...
P2374	6	4	69	36	9	30	48	53	8	19	32	58	81	25	15	27
P2909	15	7	88	50	18	49	67	...	17	21	44	...	...	28	29	45
HD 36235	...	...	44	15	...	12	27	30	...	8	11	32	41	9	...	...
HD 294269	15	8	97	44	17	58	66	74	...	31	49	66	75	29	38	32
HD 294297	...	...	58	27	6	17	33	42	9	...	15	48	58	14	9	18
HD 294302	13	...	75	39	...	24	46	50	...	15	25	67	82	...	...	...
Ceres	11	7	75	39	15	36	56	66	13	21	37	68	85	25	18	34
η Cas	8	4	58	24	9	28	40	44	5	11	22	42	62	17	10	19

TABLE 5

Fe II Equivalent Width Measurements (mÅ)

Star	Wavelength (Å)					
	6084	6149	6239	6247	6446	6456
P1037	19	23	10	36	...	46
P1158	...	22	...	37	...	46
P1199	17	28	7	48	...	57
P1455	...	...	...	...	...	...
P1467	37	56	27	78	...	82
P1474	49	56	30	94	10	93
P1590	16	21	11	48	...	56
P1657	28	39	...	cr	...	78
P1662	28	34	8	61	...	66
P2125	23	38	12	68	9	73
P2267	33	48	22	68	6	74
P2339	32	44	14	66	5	93
P2374	38	52	22	65	9	76
P2909	26	36	14	53	4	67
HD 36235	20	45	15	...	...	72
HD 294269	23	29	cr	46	...	66
HD 294297	...	...	...	...	...	77
HD 294302	53	68	...	96	...	95
Ceres	24	41	14	64	5	68
η Cas	20	34	11	52	4	59

and a significant difference in the Fe abundances from Fe I and Fe II lines. Blackwell et al. conclude that "existing numerical [theoretical] and empirical model atmospheres would therefore appear to be inadequate."

This conclusion is contested by Holweger et al. (1995), whose selection of Fe I lines with accurate laboratory *gf*-values does give the meteoritic abundance. In their analysis with the Holweger-Müller atmosphere, Fe I and Fe II lines give the meteoritic abundance to within the small errors of measurement. Holweger et al. claim to have identified reasons why Blackwell et al. (1995) obtain a higher abundance from their selection of Fe I lines.

If, as seems plausible, the model solar atmospheres are defective to the degree that abundance differences or systematic errors of about ± 0.1 dex may be introduced, it behooves us to check the solar *gf*-values against accurate laboratory values now available for many lines. An assessment of the laboratory *gf*-values was provided by Lambert et al. (1995). The more accurate values (grade A) are, in general, contributed by the Oxford furnace and the lifetime/branching ratio experiments; see the above-cited papers on the solar Fe abundance for references to the experimental results. Less accurate results (grade B) include those provided by arcs and shock tubes. Following the precepts discussed by Lambert et al., we assembled a list of laboratory measurements and checked them against our solar values of log *gf*. For the 19 grade A lines with a solar *gf*-value in Table 3, we find that the laboratory log *gf* values are effectively the same as the solar values, with a mean difference and standard deviation of 0.00 ± 0.06. Eleven grade B lines have similarly small differences: the mean difference is 0.03 ± 0.04, with our solar *gf*-values being somewhat smaller. Therefore, use of these 30 Fe I laboratory *gf*-values with the Kurucz model would give the Fe abundance as log ϵ(Fe) = 7.51 + 0.01 = 7.52, which is within 0.05 dex of Blackwell et al.'s (1995) estimate for the theoretical model, but from a different selection of lines, etc. Solar *gf*-values for Fe II lines are insensitive to the choice of model atmosphere; Blackwell et al.'s (1995) analysis of Fe II lines using the Holweger-Müller and Kurucz models shows a difference in log *gf* of less than 0.01 dex. The solar Fe II *gf*-values in Table 3 agree within about 0.03 dex with the values recommended by Lambert et al. (1995), who claim their absolute scale is likely accurate to ± 0.05 dex.

Clearly, stellar abundances expressed in the customary form as [Fe/H] will be subject to a possible systematic error of up to about ± 0.1 dex. For example, adoption of the meteoritic Fe abundance and the use of the laboratory Fe I *gf*-values for the stellar analyses would increase our derived [Fe/H] estimates by about 0.00–0.03 dex. We have elected to use solar *gf*-values derived from a theoretical model of the same family as those used for the stars, in the expectation that deficiencies in the model and other assumptions (e.g., LTE) will be minimized.

4.2. *Stellar Parameters and Microturbulent Velocities*

The effective temperatures of the stars in this paper have been determined spectroscopically, by means of Fe I lines in the observed spectra (§ 3.1). Iron is a good element to use in order to constrain and define $T_{\rm eff}$, log g, and ξ, as there is a relatively large number of visible transitions from both Fe I and Fe II which span a range in excitation potential and line strength. We have estimated the temperatures for the stars which had measurable Fe lines (slow rotators) by searching for that temperature which produced zero slope in the diagram of Fe abundances versus spectral line excitation potential. In Figure 7 (*top panel*), we show the constructed diagram of abundance versus excitation potential for HD 36235. The effective temperatures derived for the program stars can be found in Table 6. We estimate that the uncertainties in the derived temperatures are of the order of 100 K: a change in $T_{\rm eff}$ by such an amount would produce a measurable change in the slope of the iron abundances versus excitation potential. We illustrate such a change in Figure 8, where the Fe I data for HD 36235 are

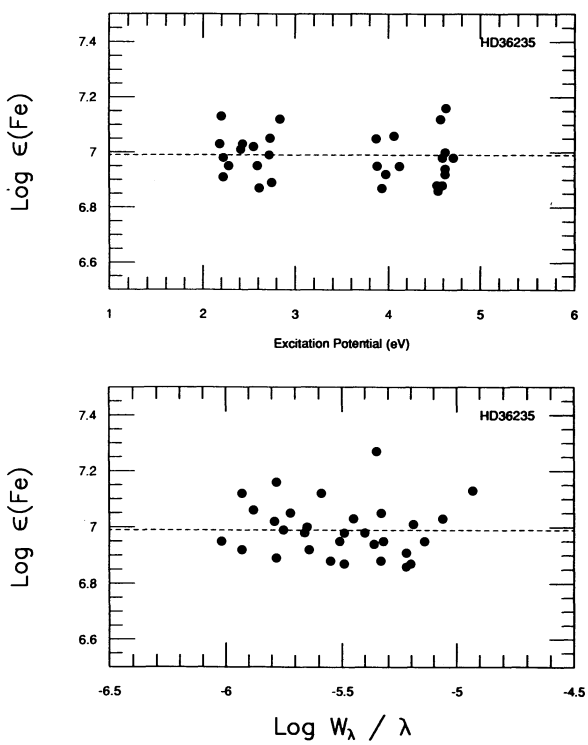

FIG. 7.—Fe abundance vs. excitation potential of the Fe I lines (*top panel*) and vs. reduced equivalent width of the measured Fe I lines (*bottom panel*) for the star HD 36235.

TABLE 6

STELLAR PARAMETERS AND ABUNDANCES

Star	T_{eff}[a] (K)	log g[b]	ξ[c]	log ϵ(Fe)	$\sigma(n)$	log ϵ(Li)	v sin i
P1037	5410	4.6	0.8	7.27	0.11 (38)	<1.0	5.0
P1158	5700	3.7	1.1	6.70	0.09 (26)	<1.2	6.0
P1179	6050*	(4.0)	(1.2)	...	...	3.3	110.0
P1199	5800	4.9	1.0	7.40	0.13 (45)	1.6	7.0
P1374	6390*	(4.0)	(1.2)	...	...	3.4	65.0
P1455	5950	(4.0)	1.5	7.59	0.15 (28)	3.5	21.0
P1467	6000	3.8	1.1	7.50	0.09 (50)	2.2	7.0
P1474	5950	4.0	1.3	7.63	0.11 (50)	1.8	7.0
P1590	6050	4.5	1.5	7.10	0.12 (43)	2.5	5.0
P1626	5530*	(4.0)	(1.2)	...	...	3.3	90.0
P1657	6100	3.8	1.6	7.20	0.14 (31)	2.6	16.0
P1662	5850	4.0	1.0	7.12	0.13 (31)	<1.3	7.0
P1789	6120*	(4.0)	(1.2)	...	...	3.2	75.0
P1953	5850*	(4.0)	(1.2)	...	...	3.3	40.0
P1955	5890*	(4.0)	(1.2)	...	...	3.4	80.0
P2125	5800	3.9	0.9	7.30	0.11 (47)	2.2	6.0
P2267	5900	4.1	0.9	7.48	0.12 (43)	2.3	4.0
P2339	5950	4.0	1.4	7.33	0.10 (46)	2.8	15.0
P2374	5900	3.9	1.3	7.41	0.09 (51)	2.3	6.0
P2909	5750	4.9	1.1	7.64	0.08 (47)	<1.2	7.0
HD 36235	6000	3.5	1.2	6.99	0.10 (31)	2.3	6.0
HD 294269	5200	4.0	0.9	7.36	0.11 (45)	<1.0	5.0
HD 294297	6150	(4.0)	1.4	7.32	0.14 (27)	2.6	5.0
HD 294298	5900*	(4.0)	(1.2)	...	...	2.6	55.0
HD 294302	6100	3.7	1.6	7.48	0.16 (32)	<1.2	8.0
η Cas	5900	4.4	1.0	7.25	0.11 (52)	2.1	6.0

[a] An asterisk indicates a photometric T_{eff}.

[b] Parentheses indicate an adopted log g; these are expected to be typical values based upon the positions of these stars in the H-R diagram.

[c] Parentheses indicate an assumed value of microturbulence.

shown for a model with $T_{eff} = 6100$ K and log $g = 3.5$: this is derived Fe abundance versus excitation potential as in the top panel of Figure 7. The dashed line illustrates the slope of Fe abundance versus excitation potential (from a linear least-squares fit), and, over the range spanned by χ, the change in derived Fe abundance between high and low excitation is about 0.1 dex, which is just at the limit of our standard deviation of the points. The mean abundance of the high-excitation lines is about 0.05 dex below the average, while the low-excitation lines yield abundances about 0.05 dex too large.

Various photometric indices can also be used to investigate the atmospheric parameters. The stars observed here in the direction of Orion are affected by varying and uncertain reddenings along the line of sight to and into the Orion region.

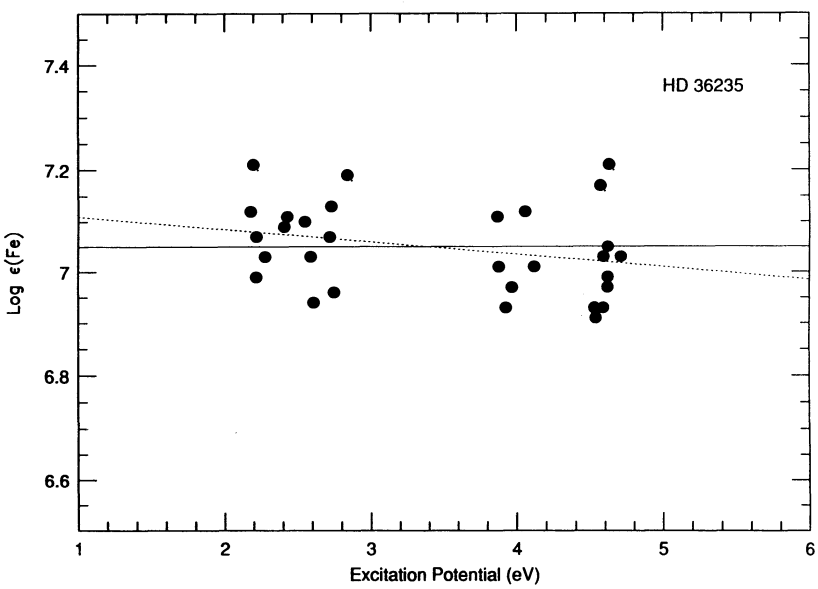

FIG. 8.—Illustration of the effect on the Fe I abundances of changing T_{eff} by +100 K for HD 36235: the solid line is the average abundance, and the dotted line is the linear least-squares fit to the points. The difference of 0.1 dex between the lower excitation and higher excitation Fe I lines is at the limit of our detection.

Nonetheless, we have estimated the effective temperatures for some of our targets by means of the available Strömgren photometry and the calibration of effective temperature and $(b - y)$ index presented in Saxner & Hammarbäck (1985). The $(b - y)$ indices for our targets were obtained from Warren & Hesser (1978) for a total of 18 stars in our list. The $(b - y)$ index is reddening dependent and needs to be corrected for the interstellar reddening. We could not find reddening estimates for most of these stars, save for five (P1374, P1590, P1657, P1789, and HD 294297). For these five stars we have derived $(b - y)_0$ indices and computed effective temperatures according to the temperature calibration in Saxner & Hammarbäck (1985). In Figure 9 we compare the temperatures derived by the two methods (photometric and spectroscopic), and we can see a reasonably good agreement between the two temperature scales for these five stars (*filled circles*): the average difference between the calibrations is Δ(photometric − spectroscopic) = 50 ± 90 K.

If we follow King's (1993) procedure, and assume an average reddening for Orion of $E(B-V) = 0.05$, we are able to compute the temperatures for the other stars with $(b - y)$ in the range for which the calibration in Saxner & Hammarbäck (1985) is valid. These stars are displayed in Figure 9 as filled triangles. We note that for these stars the agreement of the two temperature scales seems much worse: the photometric temperatures exceed the Fe spectroscopic temperatures by about 300 K. The discrepancy may come from the fact that the adopted average reddening for Orion exceeds the true reddening for these stars. This should certainly be the case if some of these stars are foreground stars. We note that the most discrepant points are assigned to be nonmembers.

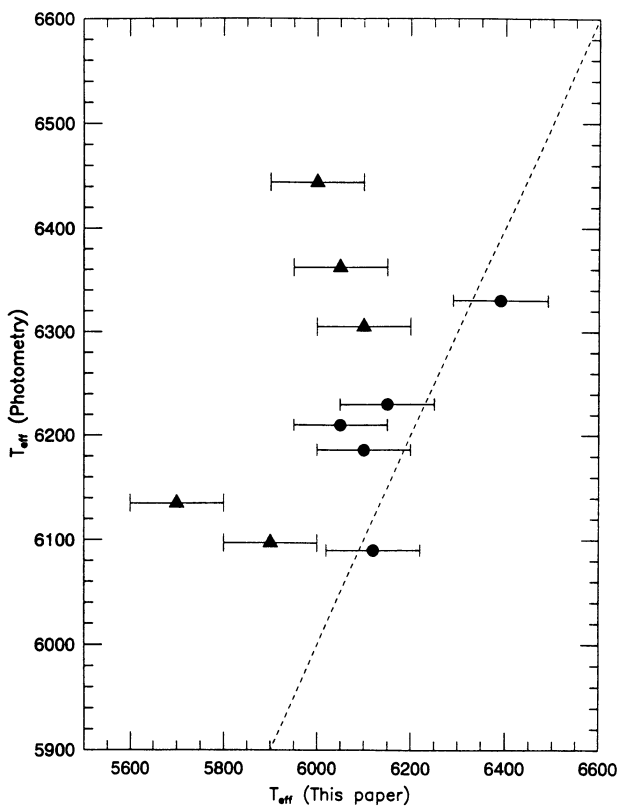

FIG. 9.—Comparison of the spectroscopic T_{eff} values derived in this paper with photometric temperatures based on the calibration by Saxner & Hammarbäck (1985). The filled circles represent stars with measured $(b - y)_0$, and the filled triangles represent the stars for which the photometric T_{eff} was derived by assuming an average reddening for Orion. The error bars represent our estimates of the uncertainties in the spectroscopic temperatures.

We will use the reddening-free Strömgren β-index to estimate T_{eff} for six of our program stars (those rotating too rapidly to have a sufficient number of detectable and unblended Fe I and Fe II lines), but only after we have calibrated the β-index using stars for which we have determined spectroscopic T_{eff} values. Our calibration of β versus effective temperature included eight stars (those which had β measurements available from the literature; Warren & Hesser 1978). The least-squares fit calculated from the points was $T_{eff} = (\beta - 1.543)/1.751 \times 10^{-4}$, with a correlation coefficient $r = 0.909$. This relation was then used to derive T_{eff} for the six stars; these T_{eff} values are marked with an asterisk in Table 6. Deviations of the spectroscopic temperatures from the fitted straight line are ± 70 K, which suggests that our internal temperature scale is consistent to roughly 70 K. This is in fair agreement with our estimate of the errors of the derived spectroscopic temperatures.

Three stars in our sample had been previously analyzed by King (1993), who derived effective temperatures from spectral-type–temperature relations, in addition to various published calibrations of photometric colors. The differences in the derived temperatures for the common stars is ΔT_{eff}(this paper − King) = 10, 60, and 50 K, respectively for P1590, P2339, and P2374. Such differences are insignificant considering that very different methods were adopted, and the estimated errors in the spectroscopic temperatures exceed these differences.

Another check on our derived temperatures comes from our analysis of the star η Cas A, which was observed as a template. Smith & Drake's (1987) detailed spectroscopic study of this star led to a $T_{eff} = 5890$ K: their determination is thus within 10 K of our derived T_{eff} for this star, which represents excellent agreement.

In the derivation of the surface gravities for the sample stars, we have searched for an agreement of the mean derived Fe abundances from Fe I and Fe II lines—the Fe II lines being sensitive to the adopted gravity. In Table 6 we present the derived values of log g for the studied stars.

The sensitivity of the strength of the Fe II lines to surface gravity, along with the typical scatter in individual Fe II lines for a single star ($\sim$0.08–0.15 dex), would yield a corresponding scatter in the log g determinations from single Fe II lines in a single star to $\pm$0.1–0.2 dex in log g. Given uncertainties in T_{eff}, a conservative estimate of the uncertainty in log g for a particular star is about 0.3 dex (the Fe II lines tend to be weak and relatively insensitive to changes in microturbulence).

An independent way to derive gravities for stars uses stellar effective temperatures and luminosities to estimate stellar masses and radii. Warren & Hesser (1978) give the V magnitudes of the stars, and with an assumed distance of 440 pc to Orion Ic, and reddening estimates, these magnitudes can be used to compute M_V, which can then be converted to M_{bol} with the addition of a bolometric correction (which is small for these stars). We assumed an average reddening for the Orion members of 0.05 mag, except for P1955, which has a measured reddening of $E(B-V) = 0.5$. The uncertainties in the reddening here, in contrast to their effect on the T_{eff} scale, do not represent a major uncertainty in the derived luminosities: a reddening of $E(B-V) = 0.05$ and an assumption of a

"normal" reddening law [$A_V = 3.3E(B-V)$] would lead to a change in the derived luminosity of only 0.07 dex. Our luminosities are found to be in good agreement with those derived by Rydgren & Vrba (1984) (for the four stars we have in common) from broadband photometry, including the infrared. The computed luminosities enable us to locate the stars in an H-R diagram (log L versus log $T_{\rm eff}$), where evolutionary tracks can be placed. An H-R diagram with PMS tracks computed by D'Antona & Mazzitelli (1994) is displayed in Figure 10. This set of tracks employed mixing-length theory in the treatment of convection and Kurucz opacities. A comparison from different sets of tracks (with different opacities and a different theory of convection) in D'Antona & Mazzitelli (1994), for the mass and temperature range we are considering, would imply differences of at most about 0.2 $M_\odot$ in the mass tracks. The stellar masses estimated from the positions of the Orion stars in this plot range from $\sim$1.5 to 2.6 $M_\odot$. The derivation of the stellar radius is straightfoward from the estimated values of $T_{\rm eff}$ and luminosity. Finally, gravities can be computed from radii and masses. Our log g values derived from the evolutionary tracks can be compared with the spectroscopic gravities adopted for the stars in this study: Δ log g(spectroscopic $-$ tracks) = 0.0 ± 0.3. We estimate the magnitude of these differences to be within the expected errors. We should note, however, that the computed luminosities and gravities make sense only if the stars examined here are true members of the Orion association; therefore, we have only examined those stars which were considered as probable members.

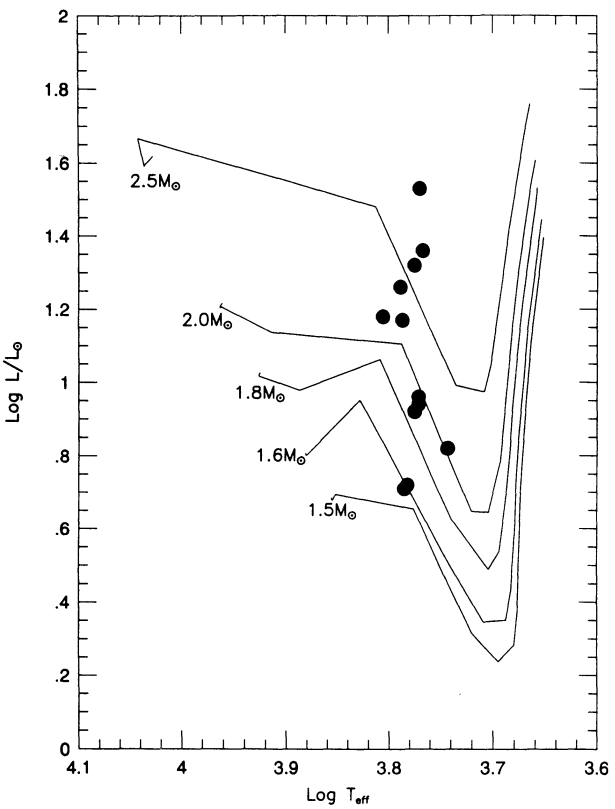

FIG. 10.—H-R diagram for the studied stars (*filled circles*) which we take to be members. The pre–main-sequence tracks were taken from D'Antona & Mazzitelli (1994). The studied stars fall in the mass range between $\sim$1.5 and 2.6 $M_\odot$.

A comparison of our spectroscopic log g values with King's (1993) estimates for the three stars in common shows a difference Δ log g(this paper $-$ King) = 0.8. 0.2, 0.1, respectively, for P1590, P2339, and P2374. The gravities in King (1993) were derived by using evolutionary tracks (from Cohen & Kuhi 1979) combining the mass and the radius estimates for these stars. The agreement between the gravities for P2339 and P2374 can be considered very good and is some additional evidence that these two are members of the association. The large discrepancy found for P1590 could be due to the fact that P1590 is not a member of the association (see § 3). For η Cas A, a comparison of our log g with the value by Smith & Drake (1987) shows perfect agreement: log $g = 4.4$. The determination in their paper is based upon fits to the wings of the infrared triplet Ca II lines, which is a completely independent method.

The microturbulence values for the sample stars were estimated by requiring that the derived Fe abundance was independent of the equivalent width of the lines. An example is shown in Figure 7 (*bottom panel*), where we plot the variation of the abundance with the reduced equivalent width [log (W_λ/λ) for one of our sample stars (HD 36235)]. The zero slope in this case was achieved for a microturbulent velocity of 1.2 km s^{-1}, where the uncertainty is estimated to be ± 0.5 km s^{-1}.

4.3. *Derived Abundances*

As discussed in § 4.1, the line-blanketed LTE model atmospheres employed in the calculations were generated with the ATLAS9 (R. L. Kurucz 1994, private communication) program for solar metallicity, an assumed depth-independent turbulence of 2 km s^{-1}, and a mixing-length parameter $\alpha = 1.25$. We have tested the model atmospheres (and abundances) against variations of the mixing-length parameter between 1.2 and 1.5, but no significant differences were found in the derived abundances.

LTE Fe abundances were derived from the equivalent widths of our selected sample of Fe I and II lines for the adopted values of $T_{\rm eff}$, log g, and microturbulence. The mean Fe abundances, the standard deviation of the mean abundances (from line-to-line scatter), and the number (n) of Fe lines are found in Table 6. For damping constants of the lines we used the Unsöld approximation (Unsöld 1955); however, most of the lines are weak enough to be insensitive to the damping parameters. Tests show that an increase of the damping constant by a factor of 6.3 changed the Fe abundances by typically less than 0.05 dex.

LTE Li abundances were derived from the fit between a synthetic and an observed spectrum in the region of the Li I doublet at 6707.8 Å. The synthetic spectrum was generated using the program MOOG (Sneden 1973), and the line list employed in the calculations was compiled from the line list of Kurucz & Peytremann (1975). All fine-structure and hyperfine-structure components of the Li doublet were explicitly included, with the wavelengths and gf-values taken from the discussion of Andersen, Gustafsson, & Lambert (1984). Also included in the synthesis were $^{12}C^{14}N$ lines, with solar abundances assumed for C and N in these dwarf stars. No ^{6}Li was included in our calculations. The line list from 6705 to 6710 Å is shown in Table 7, where we list the wavelength, species identification, excitation potential, and gf-value. The synthetic spectra were broadened to account for the instrumental profile and also stellar rotation. The v sin i values for the stars were estimated from the best fit between the observed and theoreti-

TABLE 7

LINE LIST

λ (Å)	Species	χ (eV)	gf	λ (Å)	Species	χ (eV)	gf
6705.174.....	^{12}CN	0.948	0.114E − 01	6707.766.....	Li I	0.000	0.618E + 00
6706.020.....	Si I	5.950	4.252E − 04	6707.816.....	^{12}CN	1.206	8.940E − 03
6706.290.....	Ti I	1.503	5.927E − 04	6707.904.....	Li I	0.000	0.185E + 00
6706.749.....	^{12}CN	0.866	0.173E − 01	6707.917.....	Li I	0.000	0.309E + 00
6707.050.....	Si I	5.954	1.999E − 04	6708.100.....	V I	1.218	4.630E − 03
6707.441.....	Fe I	4.610	8.112E − 03	6708.375.....	^{12}CN	2.104	1.060E − 02
6707.464.....	^{12}CN	0.792	0.973E − 03	6708.755.....	Ti I	3.922	0.808E + 00
6707.521.....	^{12}CN	2.169	3.730E − 02	6708.967.....	^{12}CN	0.887	0.182E − 01
6707.529.....	^{12}CN	0.956	0.246E − 01	6709.064.....	^{12}CN	0.820	0.683E − 02
6707.529.....	^{12}CN	2.009	1.642E − 02	6709.603.....	^{12}CN	0.976	0.121E − 01
6707.529.....	^{12}CN	2.022	1.642E − 02	6709.610.....	Zr I	0.510	4.013E − 04
6707.563.....	V I	2.743	2.950E − 02	6709.870.....	Ca I	2.930	5.565E − 04
6707.644.....	Cr I	4.208	7.240E − 03	6709.887.....	^{12}CN	0.837	0.697E − 02
6707.754.....	Li I	0.000	0.371E + 00				

cal spectra. The derived v sin i values are listed in Table 6. Given the resolution and the S/N of our spectra, we estimate the uncertainties in the derived v sin i values to be roughly ± 5 km s^{-1}. Sample syntheses are presented in Figure 11 for three stars in our list: P1455, P1953, and P2374.

Our derived LTE Li abundances for the stars, to the nearest 0.1 dex, are presented in Table 6. Inspection of this table indicates that the Li abundance for the studied stars in the direction of Orion span a range between log ϵ(Li) = 3.5 down to our limit of detectability [log ϵ(Li) < 1.0]. The upper limit we estimate for the solar Li abundance from the Ceres spectra is log ϵ(Li) < 1.2, in agreement with the accepted Li abundance for the Sun: log ϵ(Li) = 1.16 (Anders & Grevesse 1989). The uncertainties in the derived abundances will be discussed in the following section.

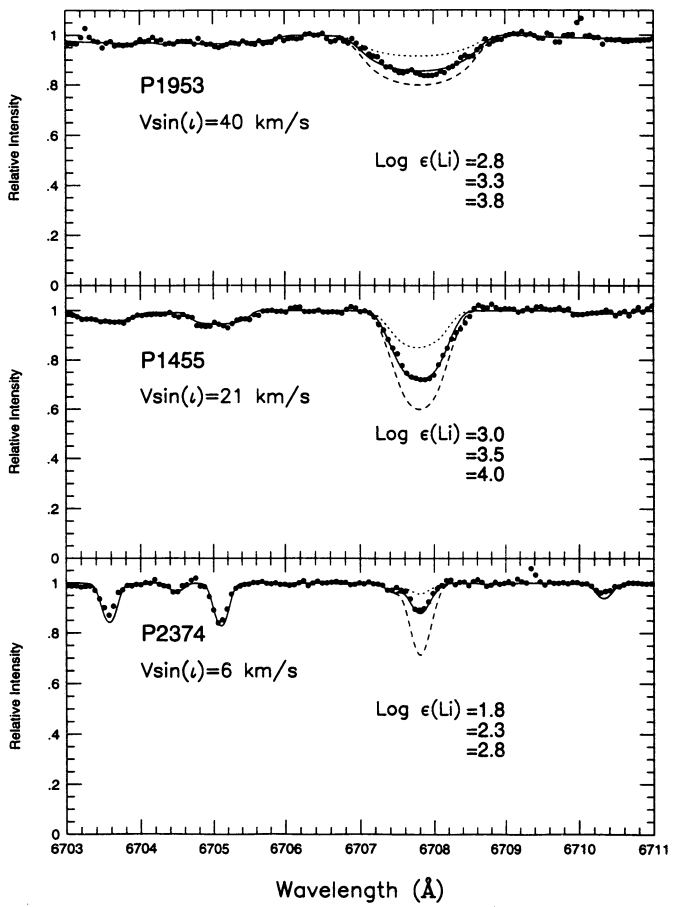

FIG. 11.—Sample syntheses of the Li doublet at 6707.81 Å for the stars P1953, P1455, and P2374. The three curves present in each panel represent three different abundances especified in the figure. All stars are considered to be members, and the three stars illustrate a range in v sin i.

4.4. *Abundance Uncertainties*

Before we turn to the discussion of the abundances presented in this paper, we need to estimate their accuracy. In this section we will start by discussing the uncertainties in the Fe abundance, and subsequently we will discuss our derived Li abundances.

Obviously, abundances can be only as accurate as the measured equivalent widths. Errors in W_λ can be due to several causes, such as errors in the data reduction procedure (e.g., inappropriate subtraction of scattered light), placement of the continuum, etc. We estimate the errors in our measured W_λ values to be of the order of a few milliangstroms. (A comparison of our equivalent width measurements for Ceres spectra with Meylan et al.'s measurements has been discussed in § 4.1.) If our Fe W_λ values are increased by 5 mÅ, the Fe abundance will be changed by from ~0.1 dex (for the 20 mÅ lines) to 0.07 dex (for the 100 mÅ lines).

Another possible source of uncertainty in the equivalent widths that needs to be discussed here is that due to the veiling of the spectral lines in young stars (especially T Tauri stars). Veiling results in a linear reduction of the observed equivalent widths of the lines due to the presence of an overlying continuum emission. We have not attempted to correct our equivalent width measurements for veiling because we contend that veiling should be a minor effect for the stars in the spectral range we are considering. This contention is based on an inspection of Table 3 in Strom, Wilkin, & Strom (1989), where the authors present their results for deveiled Li equivalent widths for a sample of stars with spectral types ranging between F6 and M3: we can see from their table that zero corrections are applied to the equivalent widths of the stars with spectral types between F6 and G7, which is the range of spectral types of our sample stars. Basri, Martin, & Bertout (1991) also list a zero veiling correction for the equivalent width of the Li line for the only star with a G2 spectral type in their list (SU Aur). We should note that because veiling correc-

tions seem to be insignificant for the Li lines, they can be assumed insignificant for the other lines in our spectra which span a relatively small range in wavelength.

The internal errors in the Fe abundances for each studied star are presented in Table 6. These errors are mainly due to errors in the W_λ measurements but are also due to errors in the *gf*-values for the lines, microturbulence, and NLTE effects, which may be of different magnitudes for the different lines. Inspection of Table 6 shows that the typical line-to-line scatter is roughly 0.1 dex.

Another source of error in the derived abundances is the choice of the stellar parameters for the stars. In order to estimate the errors due to $T_{\rm eff}$, log g, and microturbulence, we have varied these by certain amounts and inspected the abundance variations: a change in $T_{\rm eff}$ by +100 K resulted in a change of the mean Fe abundance of +0.04 dex; a change in log g of +0.4 dex resulted in an abundance change (of the Fe I lines) of −0.02 dex. The abundance of the Fe II lines is sensitive to log g, and, as discussed before, these were used to estimate the gravities. The sensitivity of the abundances to microturbulence depends on the strength of the lines: strong lines are more sensitive to microturbulence than weaker lines. In order to estimate the sensitivity of our mean Fe abundances to the microturbulence parameter, we have varied our adopted value of microturbulence for a given star by +0.5 km s^{-1}, and the typical variation in the mean Fe abundance was −0.09 dex; changing the microturbulence by −0.5 km s^{-1} produced a typical variation in the mean Fe abundance of +0.05 dex; as expected, the variation of the microturbulence is nonlinear with the abundance variation.

Based on the discussion presented above, if we then assume typical errors for the measured W_λ values, and effective temperatures, gravities, and microturbulences of 5 mÅ, 100 K, 0.4 dex, and 0.5 km s^{-1}, respectively, we can combine these error estimates (on the assumption that they are independent) to obtain an expected error of ±0.14 for the derived Fe abundances.

As mentioned before, the Li abundances in this paper were estimated from spectrum synthesis of the Li doublet and not from equivalent width measurements. The Li abundances are most sensitive to the choice of effective temperatures: a change in $T_{\rm eff}$ of 100 K would imply a Li abundance variation of 0.08 dex. But, on the other hand, the Li abundances are almost insensitive to changes in the gravities and microturbulence: a change in log g of 0.5 dex has virtually no effect on the Li abundances, nor do variations in the microturbulence of 0.5 km s^{-1}. Therefore, the expected errors in the Li abundances are dominated by the uncertainties in the derived effective temperature.

4.5. *Non-LTE Effects*

Throughout this abundance analysis we have assumed LTE in deriving abundances, and the validity of this assumption for the specific cases of Fe I, Fe II, and Li I can be checked using the available literature.

In a recent analysis of iron in the Sun, Holweger et al. (1991) quote Steenbock's (1985) extensive calculations for Fe I and II (discussed in some detail by Holweger 1988) that imply typical non-LTE corrections for Fe I lines from −0.02 to +0.06 dex, depending on the excitation potentials and equivalent widths. As the stars analyzed here do not differ very much from the Sun in the critical parameters of $T_{\rm eff}$, log g, and metallicity, these results indicate that non-LTE effects in our sample of Fe I lines are small and are masked by the uncertainties in the equivalent width measurements and *gf*-values. Holweger's (1988) discussion of Steenbock's (1985) predictions for Fe II indicate that the non-LTE effects are even smaller for Fe II lines.

Concerning Li I, we use the recent tables of non-LTE corrections from Carlsson et al. (1994) to estimate the effects on our derived Li abundances. Over our temperature and gravity range, for the lower Li abundances where log ϵ(Li) $\leq$ 2.5, the non-LTE corrections range from just −0.05 to +0.01 for the weaker Li I lines [in the sense of Δ(correction) = log $\epsilon_{\rm non\text{-}LTE}$ − log $\epsilon_{\rm LTE}$]. For the stronger Li lines the non-LTE corrections are larger. For solar-metallicity models at log g = 4.0, the non-LTE corrections are −0.17 at $T_{\rm eff}$ = 6500 K, −0.24 at 6000 K, and −0.31 at 5500 K [log ϵ(Li) $\approx$ 3.5]. We note that Carlsson et al.'s (1994) non-LTE calculations are carried out using a grid of models generated by the MARCS code (Gustafsson et al. 1975), whereas our LTE abundances are based upon ATLAS9 models, thus we ignore any differences between the two sets of models. In Table 8 we present the non-LTE corrections and the calculated non-LTE abundances for the Orion members. These abundances will be discussed in § 5.

5. DISCUSSION

This discussion looks initially at the lithium abundances of the association members and nonmembers. By our criteria for membership in the association, 10 stars in the sample are deemed to be members and two are considered probable members (Table 5): subgroup Ib is reresented by the two probable members, Ic by eight members, and Id by two members. Iron abundances are available for four members and one probable member, as well as for 13 nonmembers. Differences in the abundances for members and nonmembers may be held to confirm the assignment of membership.

5.1. *The Iron Abundances and Membership*

Iron abundances were not derived for six of the members and one probable member, because these particular stars were rotating so rapidly that a sample of relatively unblended, measurable Fe I and Fe II lines was not available. In a future paper we will discuss a wide sample of different elemental abundances in the Orion members, and in this future work we will

TABLE 8

NON-LTE CORRECTIONS AND ABUNDANCES

Star	$\Delta_{\rm (non\text{-}LTE-LTE)}$	log ϵ(Li)	Star	$\Delta_{\rm (non\text{-}LTE-LTE)}$	log ϵ(Li)
P1179.....	−0.17	3.13	P1953.....	−0.19	3.11
P1374.....	−0.16	3.24	P1955.....	−0.22	3.18
P1455.....	−0.24	3.26	P2339.....	−0.06	2.74
P1626.....	−0.23	3.07	P2374.....	0.00	2.30
P1657.....	−0.04	2.56	HD 294297.....	−0.04	2.56
P1789.....	−0.14	3.06	HD 294298.....	−0.03	2.57

attempt to extract accurate Fe abundances for the rapid rotators. This will necessitate extensive and careful spectral syntheses for a large number of spectral regions, and, since one aspect of this present study is to identify the Orion members (using published proper motions, X-ray detections, our derived V_r and $v \sin i$ values and Li abundances), we defer these more difficult members to a future study. The derived Fe abundances are plotted as a function of $T_{\rm eff}$ in the top panel of Figure 12, where those stars considered to be members and probable members are represented by filled circles and squares, respectively, and the nonmembers by open triangles. It seems clear that the nonmembers show a larger spread in Fe abundance. We note also that there is no significant trend in the Fe abundances with effective temperature, which is an indication that no major problems exist in our adopted $T_{\rm eff}$ scale.

Our earlier studies (Cunha & Lambert 1992, 1994) of several elements from carbon to iron in B-type main-sequence stars show that the spread in composition across the Orion association is fairly small (although the O and Si abundances may show some evidence of local enhancements). An LTE analysis of Fe III lines found the Fe abundances to scatter over about ± 0.15 dex, a range set by the measurement errors in the B stars (all of which are Orion members). For the F and G stars, on the other hand, the sample of our nonmembers has Fe abundances running from 6.78 to 7.62, and, hence, the Fe abundances support our designation of some of these stars as nonmembers. For the four association members for which an Fe abundance was determined (P1455, P1657, P2339, and P2374), the mean Fe abundance is log ϵ(Fe) = 7.39 $\pm$ 0.13. The standard deviation seems consistent with the estimated errors of measurement discussed in § 4.4. The mean and standard deviation are reduced by only 0.01 dex if the possible member (HD 294297) is included. This Fe abundance overlaps the mean Fe abundance for Ic stars of 7.47 $\pm$ 0.10 derived by Cunha & Lambert (1994) from their LTE analysis of Fe III lines in B stars. The uncertainty does not include a contribution from the *gf*-values, which are likely more uncertain for the Fe III lines than for the Fe I and Fe II lines used here.

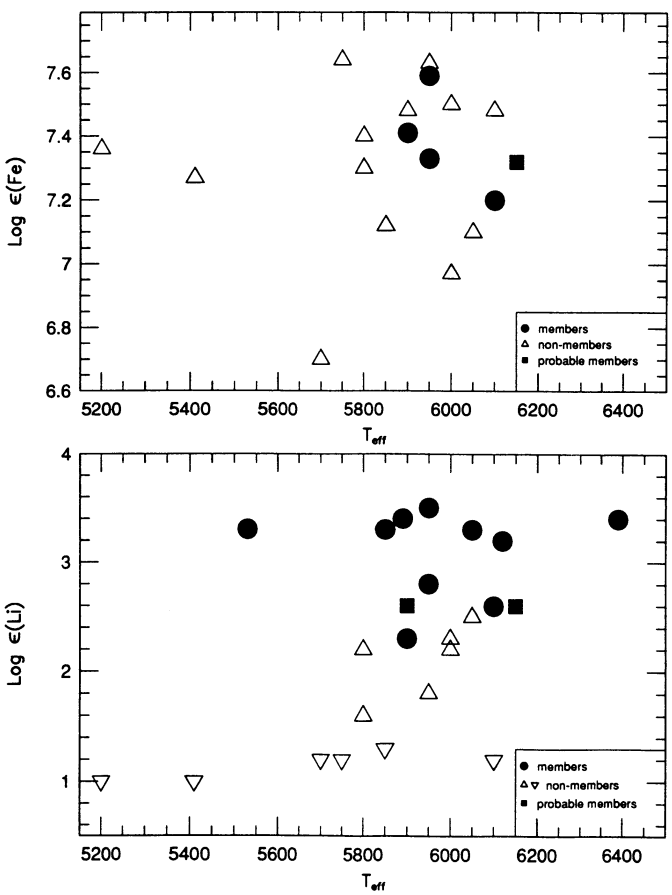

FIG. 12.—Variation of the Fe and Li abundances vs. $T_{\rm eff}$ for the observed stars. The filled circles represent the Ic and Id members, the filled squares are probable members of the Ib subgroup, and the open triangles are field stars. For the panel of Li abundances (*bottom panel*), the open triangles pointed downward represent upper limits to the Li abundance in some of the field stars.

5.2. *The Lithium Abundances*

Lithium abundances of Orion members show a small spread. In Figure 12 (*bottom panel*) we show the Li abundances as a function of $T_{\rm eff}$: filled circles and squares represent members and probable members, and open triangles nonmembers. The inverted triangles represent nonmembers with estimated upper limits for the Li abundance. The mean LTE Li abundance for the 10 Orion Ic and Id members is log ϵ(Li) = 3.1 $\pm$ 0.4, with the two possible members from subgroup Ib having a lower abundance [log ϵ(Li) = 2.6]. Among the members, three appear to have a distinctly lower Li abundance than the majority: log ϵ(Li) = 2.3, 2.6, and 2.8, but log ϵ(Li) = 3.4 $\pm$ 0.1 for the other seven stars. Since Li destruction in stars is much more likely than Li production in or on stars, we suppose the Li abundance of the seven most Li-rich stars is a measure of the association's present Li abundance. If the minority are members, as we argue, then either Li was less abundant in the interstellar gas from which these stars formed or the stars have depleted Li by a factor of 4–10. We think it unlikely that the low abundances can be attributed to a misassignment of the $T_{\rm eff}$ values; an underestimate of $T_{\rm eff}$ by well in excess of 1000 K is needed to raise the low abundance of log ϵ(Li) = 2.3 close to the mean of log ϵ(Li) = 3.4, and such an increase would also raise the Fe abundance by more than about 0.7 dex and make these stars quite metal-rich relative to the other seven. Two of the three stars with a low Li abundance are P2339 and P2374, whose membership is based on radial velocity and the detection of X-rays but which have proper motions somewhat larger than 6 mas yr^{-1}. As a final note concerning the membership question of those two stars, we note that P2339 has $v \sin i$ = 15 km s^{-1} (larger than any of the obvious nonmembers), while the two stars have (within our uncertainties) identical Fe abundances, with a difference of 0.08 dex. (It is tantalizing to note that the two possible Ib members have a lower Li abundance than the majority of Ic and Id members.)

Additional information on the Orion Li abundances is obtained by adding the results provided by King (1993), who derived abundances for 17 stars considered to be members of the Ic subgroup and for an additional six stars for which membership was deemed "possible" or "doubtful." (Among the "possible" members are P2339 and P2374, considered by us to be members.) King's spectra were of much lower resolution (about 1 Å) than ours. For the three stars in common, the Li abundances agree well: log ϵ(Li) differs in the sense (this paper – King) by only -0.1, 0.0, and 0.2 dex. If King's Li abundances were added to Figure 12, a trend of increasing abundance with decreasing $T_{\rm eff}$ would appear, as was noted by King, who was inclined to attribute the trend to a depletion of

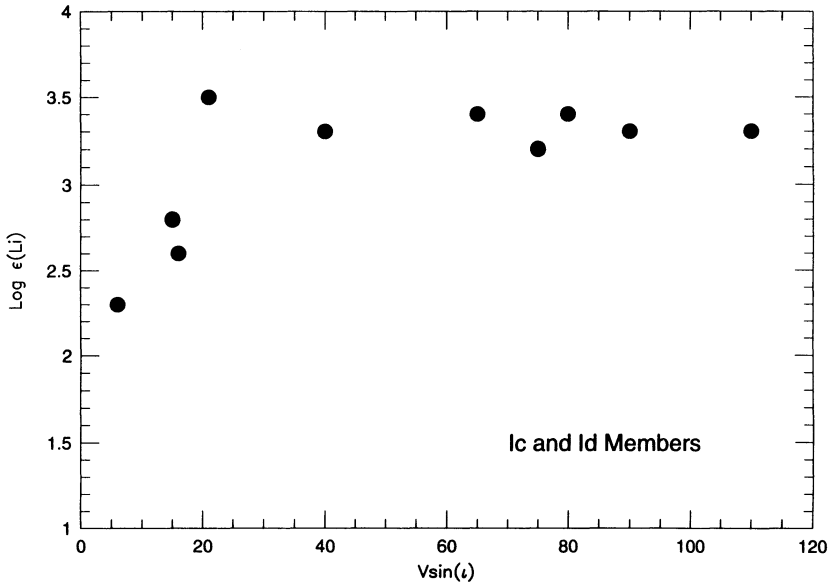

FIG. 13.—Derived LTE Li abundance vs. projected rotational velocity for the stars considered to be Ic and Id members. Note that the three stars with $v \sin i \leq 20$ km s^{-1} have lower Li abundances. Note also the small spread (≤ 0.1 dex) in Li abundance for the members with $v \sin i \geq 20$ km s^{-1} [log ϵ(Li) = 3.4].

Li in the hotter stars. The mean Li abundance from the 17 members is log ϵ(Li) = 3.6 $\pm$ 0.4 according to King, in agreement with our result. We note, however, that we have obtained a spectrum of the star from King's (1993) sample with the largest Li abundance [P1817 with log ϵ(Li) = 4.4], and we find a somewhat smaller Li I equivalent width than King: we measure W_λ = 420 mÅ for Li I in P1817, whereas King finds W_λ = 590 mÅ. This star is cool ($T_{\rm eff}$ = 4700 K), and the Li I feature may vary in strength. If our equivalent width is used in King's figure of equivalent width versus $T_{\rm eff}$, an abundance nearer to log ϵ(Li) $\approx$ 3.0–3.3 is inferred. Any trend of increasing Li abundance with decreasing temperature must be scrutinized carefully, since the Li I line is very strong in the cooler stars and the Li I feature may vary in strength.

Both analyses are LTE analyses. As we noted in § 4.5, corrections for non-LTE effects were estimated from Carlsson et al. (1994; see also Magazzu, Rebolo, & Pavlenko 1992). Applied to our stars, the non-LTE corrections lower the mean abundance by about 0.2 dex to log ϵ(Li) = 3.2 $\pm$ 0.1 for the seven members which are rapidly rotating (Table 7). The non-LTE corrections for a given Li abundance increase with decreasing $T_{\rm eff}$, so that the trend in King's sample for Li to have a higher abundance in cooler stars is lessened on application of the non-LTE corrections. The non-LTE Li abundance of the association, as provided by the seven most Li-rich members, appears almost the same as the solar system value [log ϵ(Li) = 3.3 $\pm$ 0.04; Anders & Grevesse 1989] based on the meteoritic Li/Si ratio and a photospheric (LTE) abundance analysis of the ratio of Si (and other metals) to hydrogen. Perhaps this indicates little or no growth in the local Galactic Li abundance.

Internal mixing driven by stellar rotation is commonly suspected as a mechanism for exposing lithium to warm protons and returning Li-depleted material to the surface. King (1993, his Fig. 4) noted the tendency for the stars with the smallest projected rotational velocity ($v \sin i$) to have the lowest Li abundances. But his result depends greatly on the six stars for which he considered membership in the association to be "doubtful" or "possible." Without these six, the trend disappears. The Li abundance versus $v \sin i$ relation for our members is shown in Figure 13; these stars are drawn from subgroups Ic and Id.

As noted above, three of the members do have a Li abundance well below the average, and Figure 13 shows that these have the lowest $v \sin i$ values of the sample of 10 stars. Of these three stars, we note that P1657 is a definite member based upon the criteria of proper motion ($\mu_T < 3$ mas yr^{-1}), radial velocity, and $v \sin i$ larger than those of the obvious nonmembers. Both P2339 and P2374 have proper motions only slightly larger than the mean for the Orion members, have values of V_r coincident with the Orion membership, and are X-ray sources. Thus, the evidence suggests that these three stars are members.

Over the range $v \sin i$ from 20 to 110 km s^{-1} there is no discernible change of the Li abundance in either our or King's sample. (The two possilbe members from subgroup Ib have the same low Li abundance but quite different $v \sin i$.) It is notable that the nonmembers, Ib stars apart, are all slow rotators ($v \sin i < 7$ km s^{-1}), with a wide dispersion in Li abundance: log ϵ(Li) from less than 1.0 to 2.4. The dispersion is consistent with their status as nonmembers.

The Orion members were shown in § 4.2 to be pre–main-sequence stars with masses of 1.5–2.6 $M_\odot$ and to be evolving to become main-sequence A and late B stars with $T_{\rm eff}$ in the range 8000–12,000 K. A comparison of the Li abundances in the Orion stars with those reported for field main-sequence A stars may provide evidence for Li depletion in the late stages of pre–main-sequence evolution. Selection of main-sequence stars must avoid the several varieties of chemically peculiar stars in the $T_{\rm eff}$ range 8000–12,000 K. Studies of Li in these relatively hot stars are rare, in part because the Li I 6707 Å doublet is weak, and in many stars the doublet is washed out by rotational broadening. Burkhart & Coupry (1991) provide Li (LTE) abundances for nine normal main-sequence stars with $T_{\rm eff}$ in the range 7300 to 9700 K. The abundances lie in the range log ϵ(Li) = 1.9–3.4. If the two lowest Li abundances are excluded, the abundances span the range 2.9–3.4 for a mean of 3.2 $\pm$ 0.2. A similar abundance is provided by stars in the young cluster α Per [log ϵ(Li) = 3.19 $\pm$ 0.04 from stars with 7000 K > $T_{\rm eff}$ >

5100 K; Balachandran et al. 1988] and the most Li-rich F-type main-sequence stars in the field (Balachandran 1990). Recall that the mean abundance of the 10 Orion members is log ϵ(Li) = 3.1 ± 0.4 or log ϵ(Li) = 3.4 ± 0.1 if three stars of low Li abundance are omitted. Then we must conclude that stars evolving from the pre–main-sequence stage of the Orion stars to the main sequence deplete lithium only slightly if at all, and any depletion appears to correlate with a slowing of the star's rotation. These comparisons are of LTE Li abundances for stars of different $T_{\rm eff}$ (and log g) analyzed with different grids of model atmospheres, with particular models selected by different criteria for $T_{\rm eff}$ and log g. Hence, small real differences in Li abundance may be masked. The conclusion that Orion's pre–main-sequence stars will lose little, if any, Li in evolving to the main sequence rests on the assumption that the initial Li abundances of Orion stars are equal to those of the comparison main-sequence stars. Certainly the upper envelope to the plot of Li abundance versus metallicity (Rebolo, Molaro, & Beckman 1988; Balachandran 1990) indicates little or no growth of the Li abundance for [Fe/H] > −0.3.

The Orion association is possibly an exceptional site for Li synthesis. Bloemen et al. (1994) detected γ-rays from excited C and O nuclei from Orion. This excitation, it is argued, signals the presence there of a flux of low-energy heavy (i.e., C, etc.) cosmic rays; the flux level may be 30 times that near the Sun. It is further argued that the flux of protons and alpha particles in the cosmic rays is not elevated above local levels. Flux levels of the low-energy heavy cosmic rays are probably not sufficiently high to synthesize Li from spallation reactions (C, N, and O on proton or alpha-particle collisions), but, since the origin of the cosmic-ray flux in the association is unknown, its temporal development is a matter of speculation, and the yield of Li is uncertain. It would appear from the Li abundances provided by us and by King (1993) that Li production within the association has not been dramatic. A better assessment will come when a detailed examination is made of lithium in all four subgroups of the association.

5.3. *Chemical Evolution of Lithium*

D'Antona & Mateucci (1991) discuss the evolution of the Galactic Li abundance in terms of theoretical models and find that their "best model" (where ^{7}Li is produced by AGB stars and novae) predicts roughly a factor of 2 increase in the disk Li abundance over the last 4.5 Gyr. Our results, both LTE and non-LTE, for the current Orion association Li abundance disagree with this particular prediction. Perhaps the Li abundance has "saturated," in the sense that net Li production is matched approximately by Li astration.

It is worth pointing out that Franco et al. (1988) have suggested that the Orion association results from star formation triggered by the impact between an infalling high-velocity cloud and the Galactic plane. This scenario is mentioned in Cunha & Lambert (1992) as a possible explanation for the somewhat low oxygen abundances ([O/H] ≈ −0.2) found for the oldest Orion B main-sequence stars: the infalling gas could be of low metallicity. Such a picture could also accommodate a Li abundance either near-solar, or somewhat below solar, even if the Galactic disk ^{7}Li abundances were still increasing, provided that the infalling gas had a lower ^{7}Li abundance, e.g., if the infalling gas had the presumed big bang abundance of log $\epsilon(^7\mathrm{Li})$ = 2.1–2.2.

The mean [Li/Fe] found for the Orion stars studied here is roughly 0.0 to −0.1 and therefore not very far from the meteoritic value. We note that this observed ratio cannot be explained exclusively by the production of Li in supernovae via neutrino-induced processes. Calculations by Timmes, Woosley, & Weaver (1995) predict a Li abundance of roughly 2.9 for the metallicity of Orion. Therefore, other sources of Li are indeed needed in order to explain the current Li abundance.

6. CONCLUDING REMARKS

Pre–main-sequence F–G stars of the Ic and Id subgroups of the Orion association have been shown to have the Li abundance, log ϵ(Li) = 3.2 ± 0.1 when non-LTE effects are considered, characteristic of other young but somewhat older clusters and the meteorites. It has been argued that completion of the approach to the main sequence will not lead to depletion of the surface Li abundance. The Li abundance appears to be independent of a star's effective temperature, but there is a hint that the more slowly rotating stars have a lower Li abundance due presumably to mixing and destruction of lithium. Our results are generally consistent with results by King (1993) from low-resolution spectra for an almost entirely different sample of Ic stars. If the Orion interstellar clouds may be regarded as representative of local Galactic gas, the near-equality of the Li abundances of Orion, other local Galactic clusters, and meteorites suggests that the Li abundance has evolved only a little over the last 5 Gyr.

A tantalizing hint was offered here that the Ib subgroup may have a lower Li abundance. This result, however, rests upon two stars whose membership in the association is considered probable but not certain. It will now be valuable to examine the Li abundances of a sample of confirmed members in the Ia and Ib subgroups in order to search for a possible growth of the Li abundance between the oldest (Ia) and the youngest (Id) parts of the association. This extension of the present work should then set limits on the production of Li by type II supernovae and by the embedded high fluxes of heavy cosmic rays.

We thank Jeremy King, Celso Batalha, Chris Sneden, and Suchitra Balachandran for many helpful conversations. This research is supported by the National Science Foundation (AST 93-15124) and the Robert A. Welch Foundation of Houston, Texas. K. C. acknowledges travel support for observing trips from CNPq-Brazil. This research has made use of the SIMBAD database, operated at CDS, Strasbourg, France.

REFERENCES

Anders, E., & Grevesse, N. 1989, Geochim. Cosmochim. Acta, 53, 197
Anderson, J., Gustafsson, B., & Lambert, D. L. 1984, A&A, 136, 75
Balachandran, S. 1990, ApJ, 354, 310
Balachandran, S., Lambert, D. L., & Stauffer, J. R. 1988, ApJ, 333, 267
Basri, G., Martin, E. L., & Bertout, C. 1991, A&A, 252, 625
Biémont, E., Baudoux, M., Kurucz, R. L., Ansbacher, W., & Pinnington, E. H. 1991, A&A, 249, 539
Blaauw, A. 1964, ARA&A, 2, 213
———. 1991, in The Physics of Star Formation and Early Stellar Evolution, ed. C. J. Lada & N. D. Kylafis (NATO ASI Ser. C), 342, 125
Blackwell, D. E., Booth, A. J., Haddock, D. J., Petford, A. D., & Legget, S. K. 1986, MNRAS, 220, 549
Blackwell, D. E., Lynas-Gray, A. E., & Smith, G. 1995, A&A, 296, 217
Bloemen, H., et al. 1994, A&A, L5
Boesgaard, A. M., Budge, K. G., & Ramsay, M. E. 1988, ApJ, 327, 389
Boesgaard, A. M., & Tripicco, M. J. 1986, ApJ, 302, L49
Brown, A. G. A., de Geus, E. J., & de Zeeuw, P. T. 1994, A&A, 289, 101
Burkhart, C. E., & Coupry, M. F. 1991, A&A, 249, 205
Carlsson, M., Rutten, R. J., Bruls, J. H. M. J., & Shchukina, N. G. 1994, A&A, 288, 860

Cayrel, R., Cayrel de Strobel, G., Campbell, B., & Dappen, W. 1984, ApJ, 283, 205
Cohen, M., & Kuhi, L. V. 1979, ApJS, 41, 743
Cunha, K., & Lambert, D. L. 1992, ApJ, 399, 586
———. 1994, ApJ, 426, 170
D'Antona, F., & Matteucci, F. 1991, A&A, 248, 62
D'Antona, F., & Mazzitelli, I. 1994, ApJS, 90, 467
Duncan, D. K., & Jones, B. F. 1983, ApJ, 271, 663
Franco, J., Tenorio-Tagle, G. Bodenheimer, P., Mözyczka, M., & Mirabel, I. F. 1988, ApJ, 333, 826
Fuhr, J. R., Martin, G. A., & Wiese, W. L. 1988, J. Phys. Chem. Ref. Data, 17, Suppl. 4
Gustafsson, B., Bell, R. A., Eriksson, K., & Nordlund, Å. 1975, A&A, 42, 107
Hannaford, P., Lowe, R. M., Grevesse, N., & Noels, A. 1992, A&A, 259, 301
Holweger, H. 1988, in The Impact of Very High S/N Spectroscopy on Stellar Physics, ed. G. Cayrel de Strobel & M. Spite (Dordrecht: Kluwer), 111
Holweger, H., Bard, A., Kock, A., & Kock, M. 1991, A&A, 249, 545
Holweger, H., Heise, C., & Kock, M. 1990, A&A, 232, 510
Holweger, H., Kock, M., & Bard, A. 1995, A&A, 296, 233
Holweger, H., & Müller, E. A. 1974, Sol. Phys., 39, 19
Jones, B. F., & Walker, M. 1988, AJ, 95, 1755
King, J. R. 1993, AJ, 105, 1087
Kurucz, R. L., Furenlid, I., Brault, J. K., & Testerman, L. 1984, The Solar Flux Atlas from 296 nm to 1300 nm (Sunspot: NSO)
Kurucz, R. L., & Peytremann, E. 1975, SAO Spec. Rep., 362
Lambert, D. L., Heath, J. E., Lemke, M., & Drake, J. J. 1995, ApJ, submitted
Magazzu, A., Rebolo, R., & Pavlenko, Y. V. 1992, ApJ, 392, 159
McCarthy, J. K., Sandiford, B. A., Boyd, D., & Booth, J. 1993, PASP, 105, 881
McNamara, B. J. 1976, AJ, 81, 375
McNamara, B. J., Hack, W. J., Olson, R. W., & Mathieu, R. D. 1989, AJ, 97, 1427
McNamara, B. J., & Huels, S. 1983, A&AS, 54, 221
Meylan, T., Furenlid, I., Wiggs, M., & Kurucz, R. L. 1993, ApJS, 85, 163
Milford, P. N., O'Mara, B. J., & Ross, J. E. 1994, A&A, 292, 276
Moore, C. E. 1945, A Multiplet Table of Astrophysical Interest (NSRDS-NBS 40)
Parenago, P. P. 1954, Publ. Sternberg. Astron. Inst., 25, 1
Rebolo, R., Molaro, P., & Beckman, J. E. 1988, A&A, 192, 192
Rydgren, A. E., & Vrba, F. J. 1984, AJ, 89, 399
Saxner, M., & Hammarbäck, G. 1985, A&A, 151, 372
Smith, G., & Drake, J. J. 1987, A&A, 181, 103
Smith, M. A., Pravdo, S. H., & Ku, W. H. M. 1983, ApJ, 272, 163
Sneden, C. 1973, ApJ, 184, 839
Steenbock, W. 1985, in Cool Stars with Excesses of Heavy Elements, ed. M. Jaschek & P. C. Keenan (Dordrecht: Reidel), 231
Strand, K. A. 1958, ApJ, 128, 14
Strom, K. M., Wilkin, F. P., & Strom, S. E. 1989, AJ, 98, 1444
Timmes, F. X., Woosley, S. E., & Weaver, T. A. 1995, ApJS, 98, 617
Unsöld, A. 1955, Physik der Sternatmosphären (Heidelberg: Springer)
van Altena, W. F., Lee, J. T., Lee, J.-F., Lu, P. K., & Upgren, A. R. 1988, AJ, 95, 1744
Vilas, F., Larson, S. M., Hatch, E. C., & Jarvis, K. S. 1993, Icarus, 105, 67
Warren, W. H., & Hesser, J. 1978, ApJS, 36, 497